American Society for Microbiology

Journal of Virology®

Pathogenic Correlates of Simian Immunodeficiency Virus-Associated B Cell Dysfunction

Egidio Brocca-Cofano,[a,b] David Kuhrt,[a,b] Basile Siewe,[c] Cuiling Xu,[a,d]
George S. Haret-Richter,[a,b] Jodi Craigo,[a,d] Celia Labranche,[e] David C. Montefiori,[e]
Alan Landay,[c] Cristian Apetrei,[a,d] Ivona Pandrea[a,b]

Center for Vaccine Research, University of Pittsburgh, Pittsburgh, Pennsylvania, USA[a]; Departments of
Pathology[b] and Microbiology and Molecular Genetics,[d] School of Medicine, University of Pittsburgh,
Pittsburgh, Pennsylvania, USA; Department of Immunology and Microbiology, Rush University Medical Center,
Chicago, Illinois, USA[c]; Duke Human Vaccine Institute, Duke University School of Medicine, Durham, North
Carolina, USA[e]

ABSTRACT We compared and contrasted pathogenic (in pig-tailed macaques [PTMs])
and nonpathogenic (in African green monkeys [AGMs]) SIVsab infections to assess
the significance of the B cell dysfunction observed in simian (SIV) and human immu-
nodeficiency virus (HIV) infections. We report that the loss of B cells is specifically as-
sociated with the pathogenic SIV infection, while in the natural hosts, in which SIV is
nonpathogenic, B cells rapidly increase in both lymph nodes (LNs) and intestine. SIV-
associated B cell dysfunction associated with the pathogenic SIV infection is charac-
terized by loss of naive B cells, loss of resting memory B cells due to their redistribu-
tion to the gut, increases of the activated B cells and circulating tissue-like memory
B cells, and expansion of the B regulatory cells (Bregs). While circulating B cells are
virtually restored to preinfection levels during the chronic pathogenic SIV infection,
restoration is mainly due to an expansion of the "exhausted," virus-specific B cells,
i.e., activated memory cells and tissue-like memory B cells. Despite of the B cell dys-
function, SIV-specific antibody (Ab) production was higher in the PTMs than in AGMs,
with the caveat that rapid disease progression in PTMs was strongly associated with
lack of anti-SIV Ab. Neutralization titers and the avidity and maturation of immune
responses did not differ between pathogenic and nonpathogenic infections, with
the exception of the conformational epitope recognition, which evolved from low to
high conformations in the natural host. The patterns of humoral immune responses
in the natural host are therefore more similar to those observed in HIV-infected sub-
jects, suggesting that natural hosts may be more appropriate for modeling the im-
munization strategies aimed at preventing HIV disease progression. The numerous
differences between the pathogenic and nonpathogenic infections with regard to
dynamics of the memory B cell subsets point to their role in the pathogenesis of
HIV/SIV infections and suggest that monitoring B cells may be a reliable approach
for assessing disease progression.

IMPORTANCE We report here that the HIV/SIV-associated B cell dysfunction (defined
by loss of total and memory B cells, increased B regulatory cell [Breg] counts, and B
cell activation and apoptosis) is specifically associated with pathogenic SIV infection
and absent during the course of nonpathogenic SIV infection in natural nonhuman
primate hosts. Alterations of the B cell population are not correlated with produc-
tion of neutralizing antibodies, the levels of which are similar in the two species.
Rapid progressive infections are associated with a severe impairment in SIV-specific
antibody production. While we did not find major differences in avidity and matura-
tion between the pathogenic and nonpathogenic SIV infections, we identified a ma-
jor difference in conformational epitope recognition, with the nonpathogenic infec-

tion being characterized by an evolution from low to high conformations. B cell dysfunction should be considered in designing immunization strategies aimed at preventing HIV disease progression.

Understanding the pathogenic interactions between the simian immunodeficiency viruses (SIVs) and the nonhuman primate hosts (NHPs) can lead to the development of new strategies to control human immunodeficiency virus (HIV) infection and prevent disease progression. Such studies may be even more meaningful if they involve comparisons between pathogenic and nonpathogenic SIV infections with regard to a given component of the immune system, to assess its potential role in shaping the outcome of SIV infection.

African NHP species that are natural hosts of SIVs generally do not progress to AIDS when infected with their species-specific SIV, in spite of high levels of chronic viral replication (1–4). The lack of disease progression in natural hosts is due not to exquisite immune responses (5–9) but to the ability of the natural hosts to maintain the T cell homeostasis through multiple mechanisms: (i) resolution of chronic immune activation and inflammation at the transition from acute to chronic infection (2, 10–18), (ii) restriction of SIV infection and preservation of critical $CD4^+$ T cell subsets (18–23), and (iii) modulation of target cell availability (18, 24, 25). These multiple host adaptations aimed at preventing the deleterious consequences of SIV infection and progression to AIDS occurred during hundreds of thousands to millions of years of coevolution between SIVs and their hosts (26–28).

In addition to the pathogenic features listed above, numerous studies recently identified various differences between pathogenic and nonpathogenic infections with regard to multiple immune cell subsets (CD4 cells, Th17 cells, regulatory T cells [Treg], myeloid dendritic cells [mDCs], mesenchymal stem cells [MSCs], natural killer T cells [NKT], etc.) (29–31). It is therefore considered that comparing and contrasting the fates of various immune effectors between pathogenic and nonpathogenic models of HIV infection will allow us to understand their contributions to the pathogenesis of AIDS (32–36).

There is a renewed interest in understanding the role of B cells in HIV infection, mostly due to the discovery of the broadly neutralizing antibodies and to the results from multiple animal studies and clinical vaccine trials demonstrating that an effective humoral immunity can prevent HIV acquisition (37–39). Although HIV/SIV do not productively infect B cells, a significant feature of the pathogenesis of HIV/SIV infection is generalized B cell dysfunction and dysregulation. Hypergammaglobulinemia, polyclonal activation, poor immune responses to pathogens and vaccine antigens, imbalance in B cell subsets, and increased B cell turnover have been associated with persistent HIV/SIV replication and represent important features of B cell dysfunction (40). Numerous studies carried out with both humans and rhesus macaques (RMs) suggested that this B cell dysfunction may play a central role in the progression to AIDS (41), through alterations of the different subsets of circulating or tissue-resident B cells (42) and low antibody (Ab) responses (43, 44). A generalized loss of memory B cells was reported to be the major characteristic of B cell dysfunction in SIV-infected RMs (45). B cells not being infected by HIV or SIV, the mechanisms of their loss are not well understood. While a large body of literature suggested a role for either the Fas pathway (46) or the programmed death 1 (PD-1) pathway in B cell exhaustion and dysregulation of B cell homeostasis (47), very little is known about B cell survival during HIV/SIV infection and progression to AIDS.

With the goal to better understand the role played by B cell immune dysfunction in the pathogenesis of SIV infection and disease progression, we compared the pathogenic SIVsab infection of pig-tailed macaques (PTMs) to the nonpathogenic SIVsab

infection of African green monkeys (AGMs) with regard to the frequency, phenotype, functionality, and antigen specificity of B cell subsets isolated from circulation and lymphoid and mucosal tissues. We also investigated the sources of B cell dysfunction by performing a systematic assessment of T follicular helper (Tfh) cells in both species. Finally, we assessed the titers of total Ig, as well as SIV-specific binding antibodies and neutralizing antibodies (NAbs), and compared the maturation of humoral immune responses in progressive versus nonprogressive hosts by analyzing the antibody avidity and conformation ratio.

We report that (i) B cell dysfunction, defined by loss of total, naïve, and resting memory B cells, occurs in the pathogenic but not in the nonpathogenic SIV infections; (ii) B regulatory cells (Bregs) increase in both pathogenic and nonpathogenic infections, but a positive correlation between their frequency and production of interleukin 10 (IL-10) can be established only in the pathogenic infection; (iii) increases in B cell activation and apoptosis are predominantly associated with progressive SIV infection; (iv) these changes do not appear to affect production of neutralizing and binding antibodies or the dynamics of antibody avidity, which are similar in pathogenic and nonpathogenic infections; (v) however, the evolution of Ab conformation ratio shows opposite trends in nonprogressive versus progressive species; and (vi) a severe inability to mount an Ab response against gp41 is associated with rapid disease progression in the PTMs.

RESULTS

To assess the role of B cells in SIV pathogenesis and disease progression, we compared and contrasted the dynamics of B cell populations from circulation, as well as lymphoid tissues (lymph nodes [LNs]) and mucosal tissues (intestine) in SIV-infected PTMs and AGMs.

Gating strategy and assessment of total B cells, B cell subsets, and Tfh CD4$^+$ T cell in uninfected NHPs. All B and T cell subpopulations were first selected by using the singlets gate to acquire the live/dead gate; then lymphocytes were gated by a side-scatter area (SSC-A) versus forward-scatter area (FSC-A) plot (Fig. 1A to C and I to K). B cells from circulation, LNs, and intestine were identified by gating on CD3^{neg} CD20$^+$ (Fig. 1D). Naive, resting, activated and tissue-like B cell populations were distinguished through the CD27/CD21-based gating strategy and nomenclature described by Titanji et al. (42): naive B cells were defined as CD27^{neg} CD21$^+$, resting memory B cells as CD27$^+$ CD21$^+$, activated memory B cells as CD27$^+$ CD21^{neg}, and, finally, tissue-like memory B cells as CD27^{neg} CD21^{neg} (Fig. 1E to G). With this approach, we showed that the frequencies of naive and memory B cell subsets in uninfected PTMs were in range of those reported for RMs (42, 44, 48–50), thus validating the accuracy of our gating strategy.

Bregs were gated on CD20$^+$ and then defined as CD24$^+$ CD27$^+$ (Fig. 1H). To identify Tfh cells, CD4$^+$ T lymphocytes from mesenteric and axillary LNs were sequentially gated on CD3$^+$ (Fig. 1L), CD4$^+$ CD8^{neg} (Fig. 1M), and then PD-1^{high} CXCR5$^+$ cells. ICOS and Bcl-6 were used to confirm their Tfh nature (Fig. 1O). Consequently, Tfh CD4$^+$ T cells were defined as CD3$^+$ CD4$^+$ CXCR5$^+$ PD-1^{high} (Fig. 1N).

We first compared the baseline levels of total B cells and B cell subsets between AGMs and PTMs. None of the differences observed between the two NHP species with regard to the absolute counts of total circulating B cells, or their frequencies in circulation (Fig. 2A) or axillary LNs and intestine (Fig. 2B), reached statistical significance. We next compared the frequencies of the B cell subsets in blood, LNs, and intestine between uninfected PTMs and AGMs. In both species and in all studied compartments, naive B cells were the most prevalent subset, followed by activated memory B cells (in circulation), resting memory B cells (in the LNs), and the tissue-like memory B cells (in the gut). The frequencies of circulating B cell subsets were very similar in AGMs and PTMs (Fig. 2C), the only notable exception being a higher number of tissue-like memory B cells in PTMs ($P = 0.0101$) (Fig. 2C). Likewise, the frequencies of B cell subsets in the LNs were similar between the two species, the only notable difference being the higher
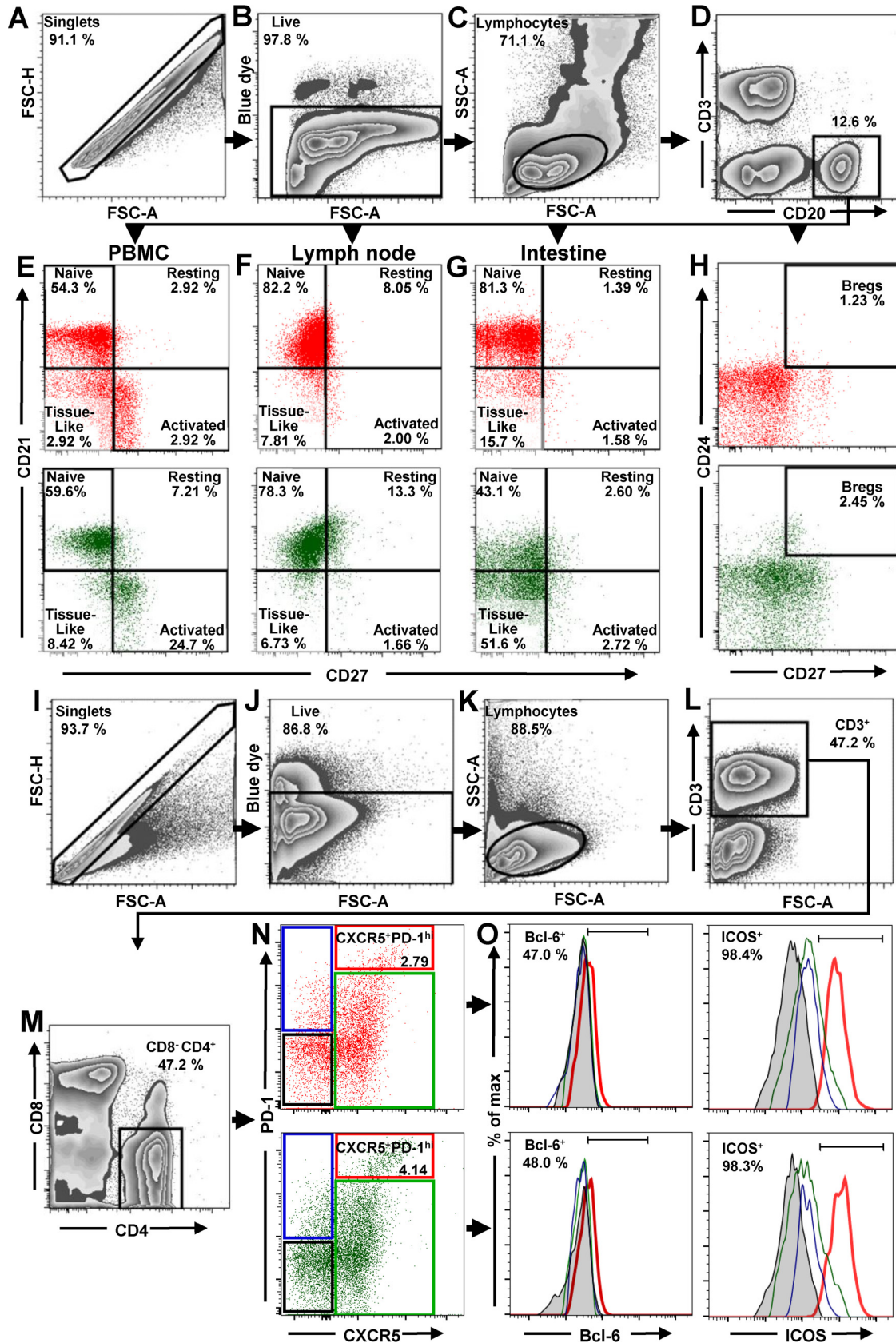
FIG 1 Flow cytometry strategy for identification of total B cells, B cells subsets, and Tfh cells in PBMCs, LNs, and intestine. The gating strategy to identify total B cells, B cell subsets, and Tfh cells in uninfected AGMs (green dot plots) and uninfected PTMs (red dot plots) is shown. Lymphocytes were gated on singlets, followed by gating on live cells (A to C). B cells from PBMCs, LNs, and intestine were

(Continued on next page)
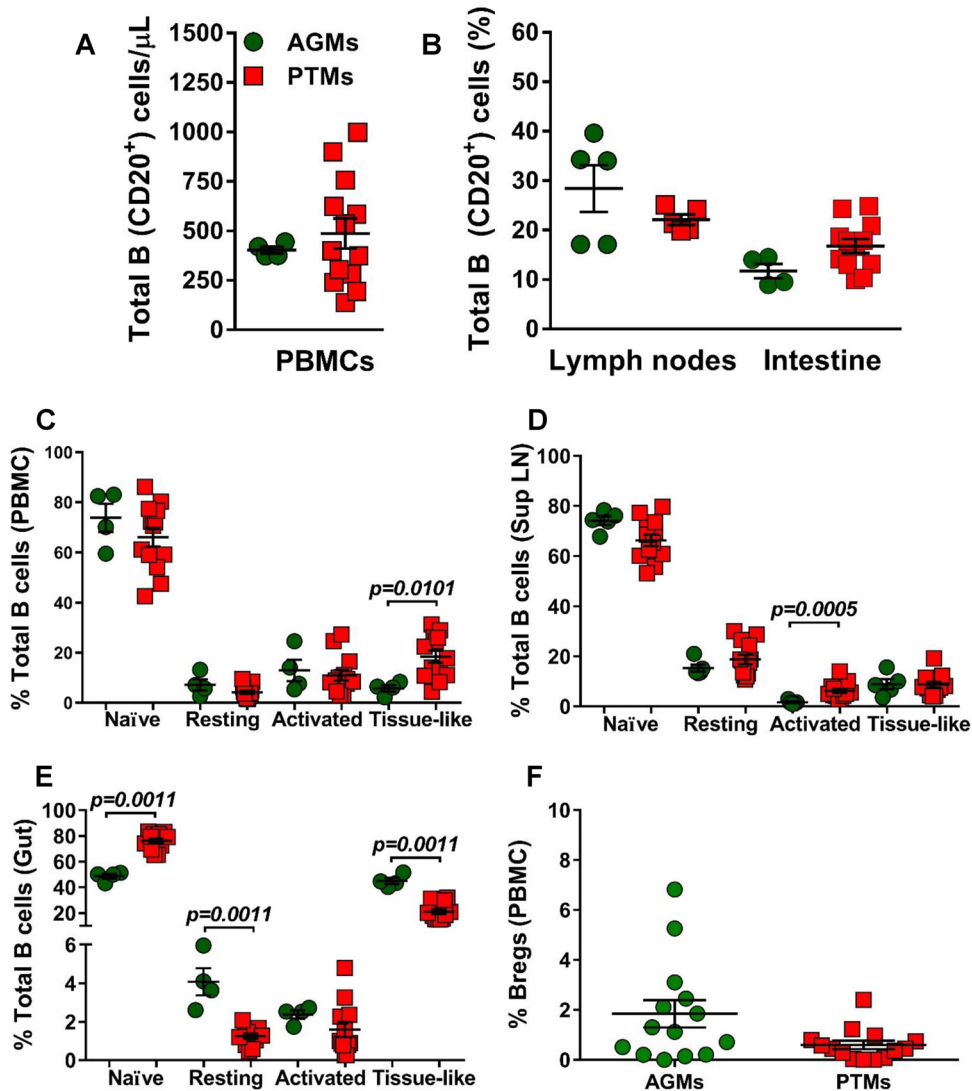
FIG 2 Total B cells and B cell subsets in peripheral blood, lymph nodes, and intestine in uninfected African green monkeys (AGMs) and pig-tailed macaques (PTMs). (A) Absolute counts of the total circulating B cells in peripheral blood (A) and frequency of total B cells in axillary lymph nodes and intestine (B). (C to E) Frequencies of the memory B cell subsets in peripheral blood (C), axillary lymph nodes (D), and intestine (E). (F) Frequency of regulatory B cells in peripheral blood. Values of individual animals are plotted, with the group means (long solid lines) and standard errors of means (short solid lines) shown. The Mann-Whitney U test was used to assess significance; P values are shown.

percentage of activated memory B cells in PTMs ($P = 0.0005$) (Fig. 2D). Significant differences between the two species were observed in the gut, where AGMs harbored significantly lower levels of naive B cells ($P = 0.0011$), while the PTMs harbored significantly lower percentages of resting ($P = 0.0011$) and tissue-like ($P = 0.0011$)

FIG 1 Legend (Continued)

selected by gating on CD20$^+$ (D). CD21 and CD27 markers were used to distinguish naive (CD27^{neg} CD21$^+$), resting memory (CD27$^+$ CD21$^+$), activated memory (CD27$^+$ CD21^{neg}), and tissue-like memory (CD27^{neg} CD21^{neg}) B cells from PBMCs (E), LNs (F), and intestine (G). CD27 and CD24 were used to identify regulatory B cells from PBMCs (H). To characterize Tfh cells in mesenteric and axillary LNs, lymphocytes were gated on singlets, followed by selection of live CD3$^+$ cells (I to L). CD4$^+$ CD8^{neg} cells were then gated (M) and analyzed based on expression of PD-1 and CXCR5. The doubly positive PD-1^{high} CXCR5$^+$ population was used to identify Tfh cells (N). Expression of Bcl-6 and ICOS was assessed in CXCR5^{neg} PD-1^{neg} CD4$^+$ T cells (black square), CXCR5^{neg} PD-1$^+$ CD4$^+$ T cells (blue square), CXCR5$^+$ PD-1^{neg} CD4$^+$ T cells (green square), and CXCR5$^+$ PD-1^{high} CD4$^+$ T cells (red square) (O). FSC-A, forward-scatter area; FSC-H, forward-scatter height; SSC-A, side scatter area.

memory B cells (Fig. 2E). We did not detect significant differences in the frequencies of circulating Bregs between the two species prior to infection (Fig. 2F).

Loss of total B cells occurs only in the pathogenic model of SIV infection. To characterize the pathogenic correlates of the B cell dysfunction, we next monitored the impact of SIVsab infection on total B cells in PTMs and AGMs (Fig. 3A to C). Very different dynamics of total B cells were observed in the two species upon SIVsab infection, with a significant loss of CD20$^+$ cells occurring rapidly in PTMs both in blood (8 days postinfection [dpi], $P < 0.0001$) (Fig. 3A) and in the LNs (4 dpi, $P = 0.0079$) (Fig. 3B). CD20 depletion also occurred in the gut during chronic infection of PTMs (72 dpi, $P = 0.0028$; >180 dpi, $P = 0.0286$) (Fig. 3C). Conversely, no significant decrease in the B cell counts could be observed at any time point and in any of the studied compartments in AGMs. Moreover, in AGMs, B cells increased early after infection in both the intestine (8 dpi, $P = 0.0286$) and the LNs (4 dpi, $P = 0.0286$), where they remained elevated throughout the follow-up (Fig. 3B). During chronic infection (after 42 dpi), there was no significant difference between PTMs and AGMs with regard to the dynamics of total B cells in either blood (Fig. 3A) or LNs (Fig. 3B).

Study of the B cell subset dynamics reveals specific patterns associated with progressive SIV infection. To assess the potential contribution of the various B cell memory subsets to disease progression, we next compared and contrasted the pathogenic and nonpathogenic models of SIV infection with regard to the dynamics of naive, resting, activated, and tissue-like memory B cell isolated from circulation, LNs, and gut (Fig. 3D to O).

An association between loss of naive B cells and disease progression could be established, supported by a consistent, significant, and rapid decrease of naive B cells in SIV-infected PTMs, documented in all three studied compartments: blood (Fig. 3D), LNs (Fig. 3E), and intestine (Fig. 3F). Conversely, in AGMs, the naive B cells decreased only slightly in the LNs during chronic infection (Fig. 3E) while increasing significantly in the gut (Fig. 3F).

Resting memory B cells were clearly depleted from circulation in SIVsab-infected PTMs throughout the follow-up (Fig. 3G), while they were transiently increased in the LN during acute infection (Fig. 3H) and consistently and massively increased in the gut throughout the follow-up (Fig. 3I).

A different pattern was observed in SIV-infected AGMs, in which circulating resting memory B cells were preserved and even increased (Fig. 3G). Resting memory B cell showed an even more prominent and significant increase in the LNs (Fig. 3H) while remaining virtually unchanged in the gut (Fig. 3I).

The frequencies of activated memory B cells dramatically increased in all three compartments in SIV-infected PTMs (Fig. 3J to L), the highest increases being observed at mucosal sites (Fig. 3L). In stark contrast, in the SIV-infected AGMs there was only a modest trend to activated memory B cell increase, reaching significance only in the LNs and only during acute infection (Fig. 3K).

In contrast to previous studies that failed to identify any significant change in the levels of tissue-like memory B cells in SIVmac-infected RMs (42, 51, 52), we found a persistent increase of this B cell subset throughout the progressive SIV infection in PTMs in all studied compartments (Fig. 3M to O). Conversely, the levels of tissue-like memory B cells did not significantly change in periphery in SIV-infected AGMs (Fig. 3M), while they were decreased in the LNs (Fig. 3N) and intestine (Fig. 3O).

Increases in the IL-10-secreting Bregs are specifically associated with pathogenic SIVsab infection. It was recently reported that Breg frequency positively correlates with markers of HIV disease progression (53–55). We therefore compared Breg frequencies and functions between uninfected and chronically SIVsab-infected AGMs and PTMs, and we report that Bregs significantly increased (14-fold) only in PTMs ($P = 0.0126$) (Fig. 4A). In AGMs, only a limited increase (2.7-fold) of Bregs was observed.

Bregs can impact cell-mediated immune responses by secreting IL-10 (56–60). Since the frequency of Bregs is very low, we measured IL-10 production by total circulating
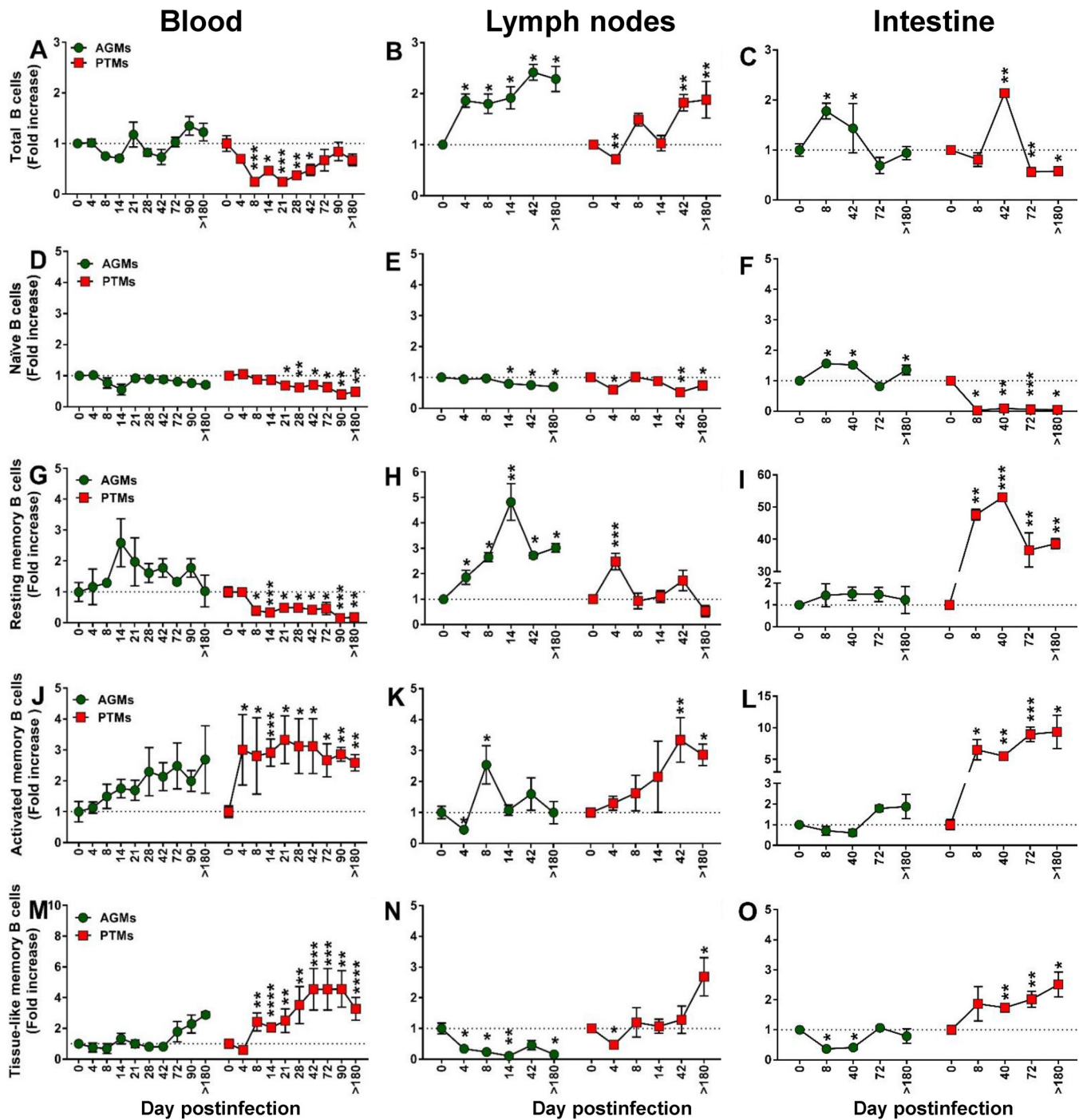
FIG 3 Changes in the total B cells as well as naive versus memory B cells from circulation, lymph nodes, and intestine over the course of progressive SIVsab infection of AGMs and nonprogressive SIVsab infection of PTMs. (A to C) Fold increase of the absolute counts of total B cells in peripheral blood (A) and in the frequency of B cells from the lymph nodes (B) and intestine (C) in AGMs and PTMs. (D to O) Fold increase of naive (D to F), resting memory (G to I), activated memory (J to L), and tissue-like memory (M to O) B cells from circulation (left), lymph nodes (middle), and intestine (right) in AGMs and PTMs. Dotted lines mark the baseline levels of total B cells and of the different cell subsets. The Mann-Whitney U test was used to assess significance. Error bars correspond to standard errors of the means. Significant changes from the preinfection baseline levels are indicated as follows: *, $P < 0.05$; **, $P < 0.01$; ***, $P < 0.001$; and ****, $P < 0.0001$.

B cells and showed that SIVsab infection induced a significant increase of the frequency of circulating total B cells expressing IL-10 ($P = 0.0451$) only in PTMs, at levels that were 2.9-fold higher than in SIVsab-infected AGMs (Fig. 4B). The IL-10 expression by total B cells positively correlated with Breg frequency ($P = 0.0064$) (Fig. 4C), strongly suggesting that the cell population expressing IL-10 is enriched in Bregs.
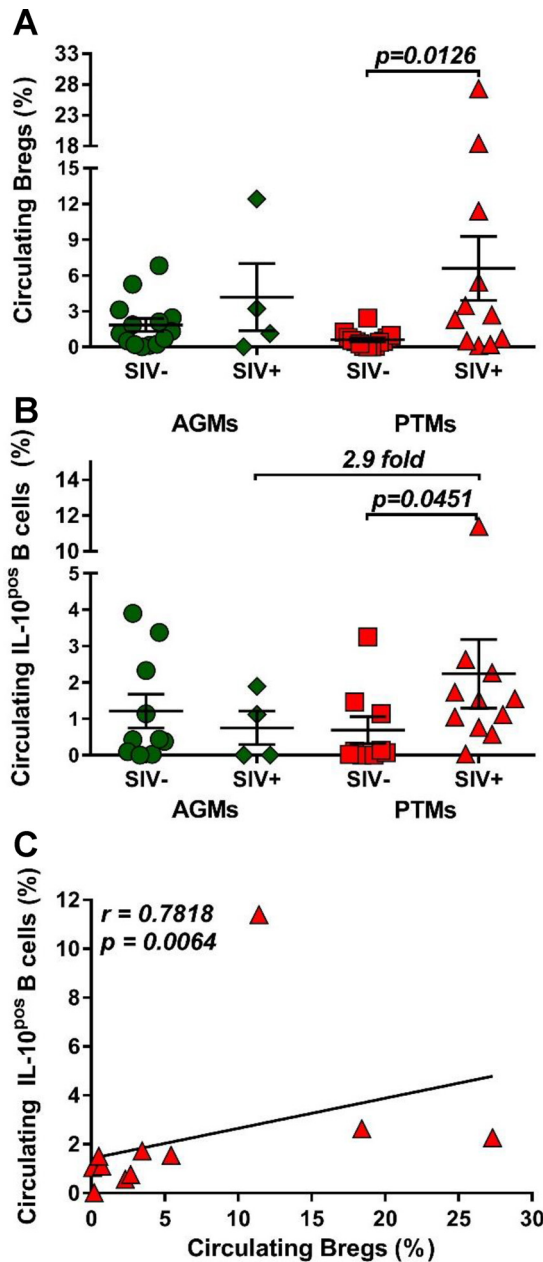
FIG 4 Frequencies of regulatory B cells and IL-10 production over the course of progressive SIVsab infection of AGMs and nonprogressive SIVsab infection of PTMs. (A) Frequencies of regulatory B cells in uninfected (green circles) versus SIVsab-infected (green diamonds) AGMs and uninfected (red squares) versus SIVsab-infected (red triangles) PTMs. (B) Expression of IL-10 in circulating total B cells from uninfected versus SIVsab-infected AGMs and uninfected versus SIVsab-infected PTMs. (C) Positive correlation between circulating total B cells expressing IL-10 and circulating Bregs in PTMs infected with SIVsab. Values of individual animals are plotted, with the group means (long solid lines) and standard errors of the means (short solid lines) shown. The Mann-Whitney U test was used to assess significance; *P* values are shown. Relationships between total circulating B cells expressing IL-10 and of the frequency of total circulating Bregs were evaluated using the Spearman rank correlation test. The significant correlation illustrated as a solid line; *P* and Spearman rank correlation (*r*) values are shown.

Dynamic expression of homing markers support B cell redistribution to mucosal sites during pathogenic SIV infection. Due to the observed depletion of the circulating B cell subsets in periphery and their increase at tissue sites, we next investigated whether the mucosal homing marker $\alpha4\beta7$ integrin is differently expressed on circulating B cells during pathogenic and nonpathogenic SIVsab infections
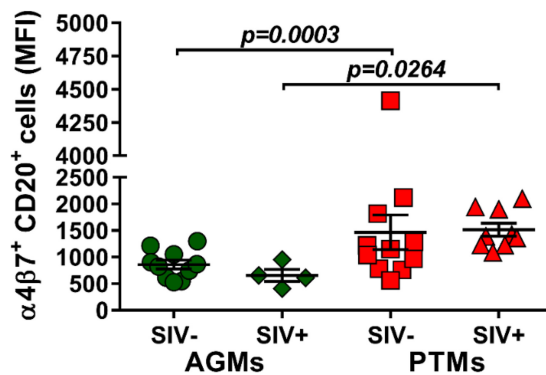
FIG 5 Mean fluorescence intensity (MFI) of $\alpha4\beta7$ integrin expression on total B cells in AGMs and PTMs. Results for uninfected (green circles) and SIVsab-infected (green diamonds) AGMs and uninfected (red squares) and SIVsab-infected (red triangles) PTMs are shown. Values of individual animals are plotted, with the group means (long solid lines) and standard errors of means (short solid lines) shown. The Mann-Whitney U test was used to assess significance; *P* value is shown.

and the potential association between B cell homing to the gut and disease progression. While $\alpha4\beta7$ integrin expression on B cells did not increase after infection in either species, the overall expression of $\alpha4\beta7$ integrin on B cells was significantly higher in PTMs than in AGMs both prior to ($P = 0.0003$) and after ($P = 0.0264$) SIV infection (Fig. 5), suggesting that the fraction of B cells homing to the gut is higher in the model of pathogenic infection.

Increased B cell apoptosis is specifically associated with pathogenic SIVsab infection. To further understand the mechanism of B cell loss during SIV infection, we assessed the frequency of apoptotic B cells throughout the follow-up in PTMs and AGMs.

The frequencies of circulating apoptotic B cells significantly increased in both species during the acute stage of infection; however, B cell apoptosis was resolved in AGMs and persisted only in chronically infected PTMs (Fig. 6A). In the LNs and intestine, the levels of apoptotic B cells remained unchanged from the baseline during the acute infection in both species but significantly increased during chronic infection in PTMs (Fig. 6B and C). The dynamics of apoptotic B cells correlated with the degree of B cell activation/proliferation (Ki-67) in both species (Fig. 7).

B cell activation is specifically associated with pathogenic SIV infection. We next interrogated whether the nonprogressive SIV infection is associated with a lack of B cell activation that parallels the control of T cell activation in these models (61). We first assessed and compared B cells isolated from circulation, LNs, and intestine from AGMs and PTMs with regard their Ki-67 expression (Fig. 8). Prior to infection, levels of Ki-67 expression on circulating B cells were similar between AGMs and PTMs (11.3% and 10.4%, respectively). Upon SIVsab infection, Ki-67 expression significantly but only transiently increased in AGMs at the transition from the acute to chronic stage of infection (Fig. 8A), differently from the T cell activation, which occurs very early after infection (62). Conversely, in SIV-infected PTMs, B cell activation increased throughout the follow-up (Fig. 8A). Ki-67 expression increased during chronic infection on the B cells from LNs, and the levels were similar in PTMs and AGMs (Fig. 8B). In the intestine, the frequency of activated B cells increased only in PTMs (Fig. 8C).

Pathogenic SIV infection is associated with increases in TLR-2. B cell activation may occur after Toll-like receptor 2 (TLR-2) stimulation (63). We therefore assessed TLR-2 expression on B cells in SIVsab-infected PTMs and AGMs and showed that while the baseline TLR-2 levels on total B cells were similar in both species, they significantly increased upon infection only in PTMs ($P = 0.0005$) (Fig. 8D).

Altogether, our results thus clearly show that chronic B cell activation is specifically associated with progressive SIV infections.
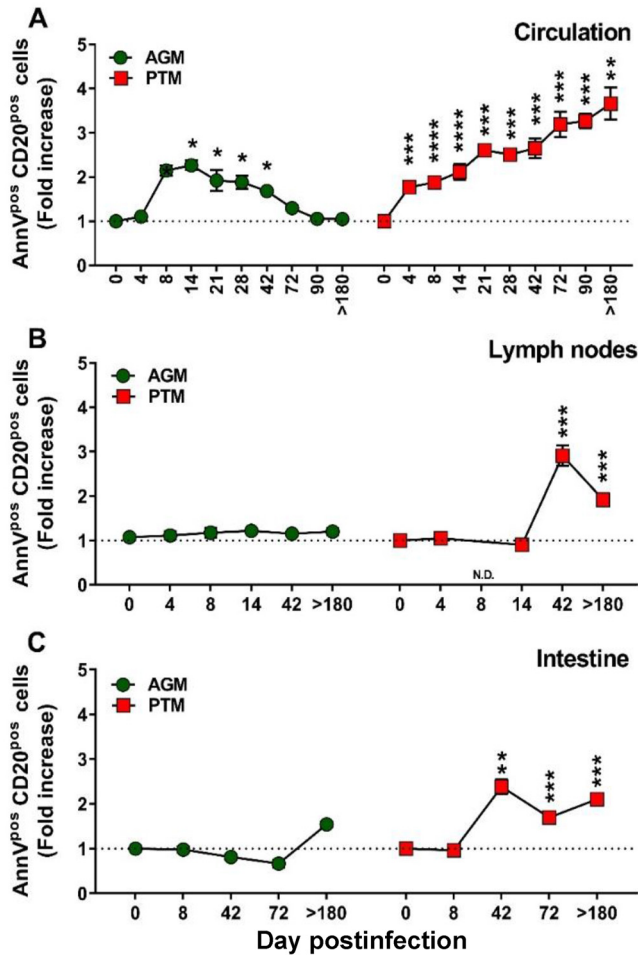
FIG 6 Changes in the levels of apoptotic B cells over the course of progressive SIVsab infection of AGMs and nonprogressive SIVsab infection of PTMs. Fold increases of the apoptotic cells from the PBMCs (A), lymph nodes (B), and intestine (C) are shown. AGMs are shown by green circles and PTMs by red squares. Dotted lines mark the baseline levels of the different cell subsets. The Mann-Whitney U test was used to assess significance. Error bars correspond to standard errors of the means. Significant changes from the preinfection baseline levels are indicated as follows: *, $P < 0.05$; **, $P < 0.01$; and ***, $P < 0.001$. AnnV, annexin V.

The frequency of Tfh cells increases during chronic SIVsab infection in pathogenic hosts. Follicular helper CD4$^+$ T (Tfh) cells are critical for generating and maintaining the immunological memory of B cell response in the LN microenvironment (64). We therefore compared the Tfh frequencies in the superficial (Fig. 9A) and mesenteric (Fig. 9B) LNs from PTMs and AGMs to assess whether differences between the two species may account for the deficiencies in B cell responses observed during the progressive infection. The gating strategy to identify the CD4$^+$ Tfh cells was based on the coexpression of CXCR5 and PD-1. Before establishing the phenotype of the CD4$^+$ Tfh cells, the doubly positive CXCR5 PD-1 CD3$^+$ CD4$^+$ T cells (Fig. 1N) were evaluated for the expression of Bcl-6 and ICOS (Fig. 1O). While only a relative small fraction of the CD3$^+$ CD4$^+$ CXCR5$^+$ PD-1$^+$ cells expressed Bcl-6 (48% in AGMs and 47%in PTMs), a larger fraction (over 98% in both PTMs and AGMs) expressed ICOS. Increases in the Tfh cell frequency were observed in chronically infected PTMs (Fig. 9A and B), while in the AGMs Tfh cells increased only transiently during the acute infection and only in the mesenteric LNs (Fig. 9B). CD4$^+$ Tfh cell increases positively correlated with the expansion of the total B cell pool only in the pathogenic infections ($P = 0.0236$) (Fig. 9C). Furthermore, Tfh cell increases also positively correlated ($P = 0.0181$) with plasma anti-gp41 antibody titers in PTMs (Fig. 9D).
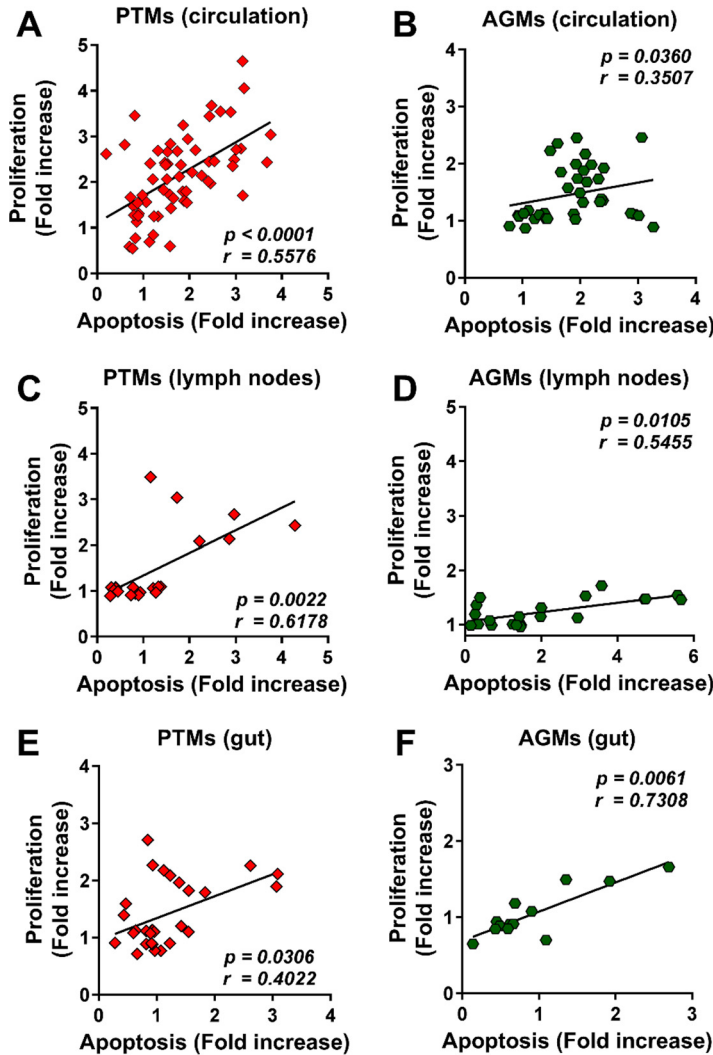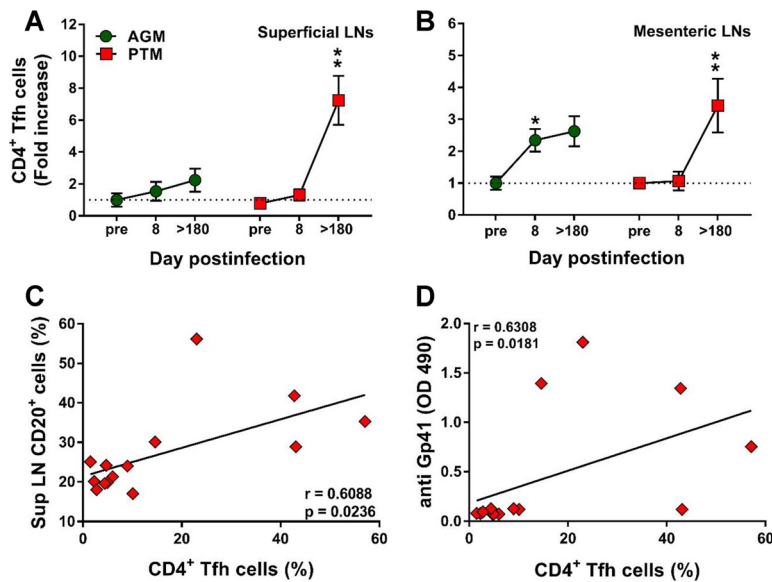
FIG 7 Correlations between proliferation and apoptosis over the course of progressive SIVsab infection of AGMs and nonprogressive SIVsab infection of PTMs. Positive correlations between proliferation and apoptosis were observed in both PTMs (red diamonds) and AGMs (green hexagons) in the blood (A and B), lymph nodes (C and D), and intestine (E and F). Relationships between proliferation and apoptosis were assessed using the Spearman rank correlation test. Significant correlations are represented by solid lines; P and Spearman rank correlation (r) values are shown.

Pathogenic species secrete significantly larger amounts of total IgG and IgA than nonpathogenic species. To assess whether the loss of total B cells in progressive species significantly impacts the overall antibody responses, we quantified the total IgG and IgA in PTMs and AGMs. Surprisingly, PTMs had higher levels of IgG and IgA than AGMs (Fig. 10A and B), in spite of the B cell loss identified in PTMs. A moderate increase of serum IgG and IgA occurred in the early phase of viral infection in both species, yet this increase reached significance only in PTMs, in which the levels of both IgG and IgA levels remained significantly increased throughout the chronic infection, from 35 dpi on. The levels of antibodies were significantly higher in PTMs than in AGMs starting from 21 dpi and 14 dpi for IgG (Fig. 10A) and IgA (Fig. 10B), respectively. We next analyzed the relationship between total antibodies and the frequency of total B cells and subsets, as well as the fraction of apoptotic and proliferating total B cells in blood and LNs in both species. In PTMs, the levels of IgG were correlated to those of total B cells from circulation (Fig. 10C) and LNs (Fig. 10D). To establish which memory B cell subset contributes most to the production of serum Abs in PTMs, we correlated the levels of total IgG and IgA with the levels of the B cell memory subsets and found a
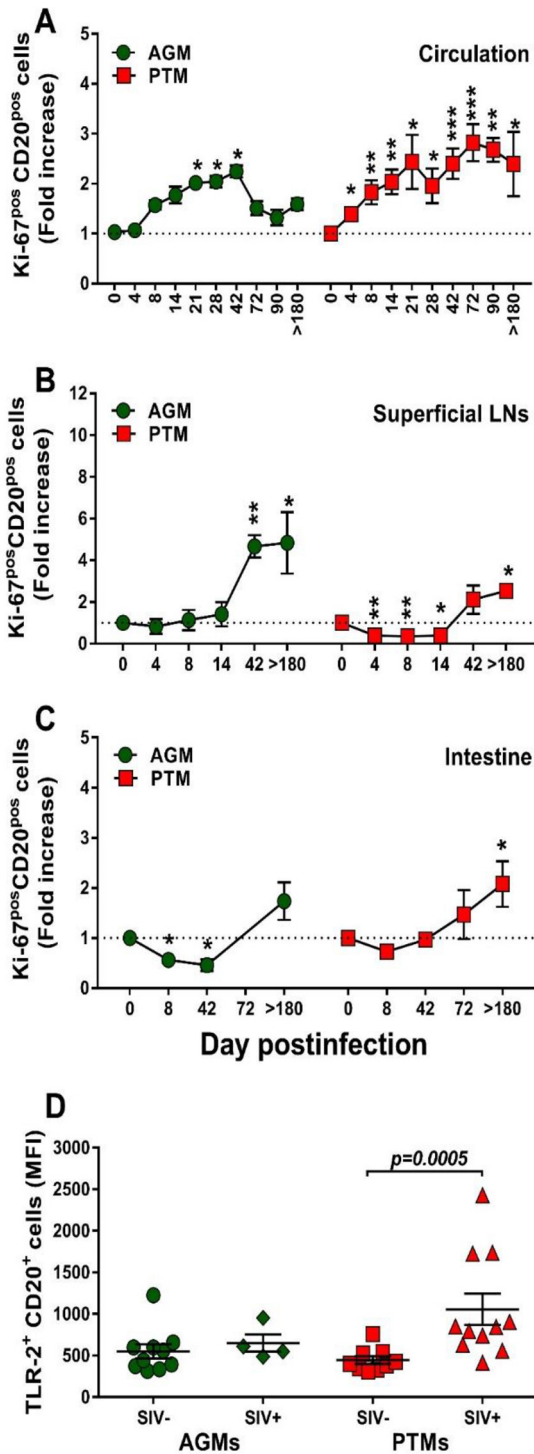
FIG 8 Changes in Ki-67 expression on total B cells over the course of progressive SIVsab infection of AGMs and nonprogressive SIVsab infection of PTMs. (A to C) Fold increase of Ki-67 expression in PBMCs (A), lymph nodes (B), and intestine (C). Dotted lines mark the baseline levels of the different cell subsets. The Mann-Whitney U test was used to assess significance. Error bars correspond to standard errors of the means. Significant changes from the preinfection baseline levels are indicated as follows: *, $P < 0.05$; **, $P < 0.01$; and ***, $P < 0.001$. (D) MFI of TLR-2 expression on total B cells over the course of progressive SIVsab infection of AGMs and nonprogressive SIVsab infection of PTMs. AGMs are shown by green circles and PTMs by red squares. Results for uninfected (green circles) versus SIVsab-infected AGMs (green diamonds) and uninfected (red squares) versus SIVsab-infected PTMs (red triangles) are shown. Values of individual animals are plotted, with the group means (long solid lines) and standard errors of means (short solid lines) shown. The Mann-Whitney U test was used to assess significance; P values are shown.

FIG 9 Changes in the levels of follicular helper CD4+ T (Tfh) cells in lymph nodes over the course of progressive SIVsab infection of AGMs and nonprogressive SIVsab infection of PTMs. (A and B) Changes in the Tfh cell frequency in axillary (A) and mesenteric (B) lymph nodes in AGMs and PTMs. Dotted lines mark the baseline levels of the different cell subsets. The Mann-Whitney U test was used to assess significance. Error bars correspond to standard errors of the means. Significant changes from the preinfection baseline levels are indicated as follows: *, $P < 0.05$; **, $P < 0.01$; and ***, $P < 0.001$. Significant differences between pathogenic and nonpathogenic species at same time point are indicated as follows: #, $P < 0.05$; ##, $P < 0.01$; and ###, $P < 0.001$. (C) Significant correlation between the frequency of total B cells and that of CD4+ Tfh cells in PTMs. (D) Significant positive correlation between frequency of CD4+ Tfh cells and the plasma levels of anti-gp-41 antibodies in PTMs. Relationships between the frequencies of B cells and anti-gp-41 antibodies versus the frequency of CD4+ Tfh cells in the axillary lymph nodes were evaluated using the Spearman rank correlation test. Significant correlations are represented by solid lines; P and Spearman rank correlation (r) value are shown.

negative correlation between naive B cells and IgG in both blood and LNs (Fig. 10E and F). Serum IgG negatively correlated with activated circulating memory B cells (data not shown) and positively correlated with the exhausted tissue-like memory B cells (Fig. 10G). In the LNs, serum IgG levels also positively correlated with activated memory B cells (Fig. 10H).

Finally, the levels of IgG correlated to those of apoptotic (Fig. 10I) and proliferating (Fig. 10K) B cells from circulation but not from the LNs (Fig. 10J and L).

Lack of anti-gp41 antibodies in rapid progressor PTMs. Using an SIVsab-specific enzyme-linked immunosorbent assay (ELISA) (65), we monitored binding antibodies to gp41 immunodominant region and found that PTMs developed significantly higher titers of anti-gp41 than AGMs (Fig. 11A). Furthermore, PTMs also developed significantly higher endpoint titers to whole Env protein than AGMs (Fig. 11C). We were not able to detect anti-gp41 antibodies in all the PTMs. Only 43% of rapid progressors (3/7) mounted a specific anti-gp41 response, as opposed to all of normal progressors (6/6) (Fig. 11B).

The neutralizing antibody titers did not differ between pathogenic and nonpathogenic SIVsab infections. Different from the dynamics of binding antibodies, PTMs and AGMs mounted similar levels of neutralizing antibodies during chronic SIVsab infection (Fig. 11D), which positively correlated ($P = 0.0311$) with the absolute total B cell counts only in AGMs (Fig. 11G). In PTMs, this trend did not reach significance (Fig. 11H).

Pathogenic and nonpathogenic hosts have opposite conformational epitope specificities. Finally, to understand the impact of B cell dysfunction on the humoral immune responses characteristic to pathogenic and nonpathogenic infections, we analyzed two critical aspects of the maturation of humoral immune responses—
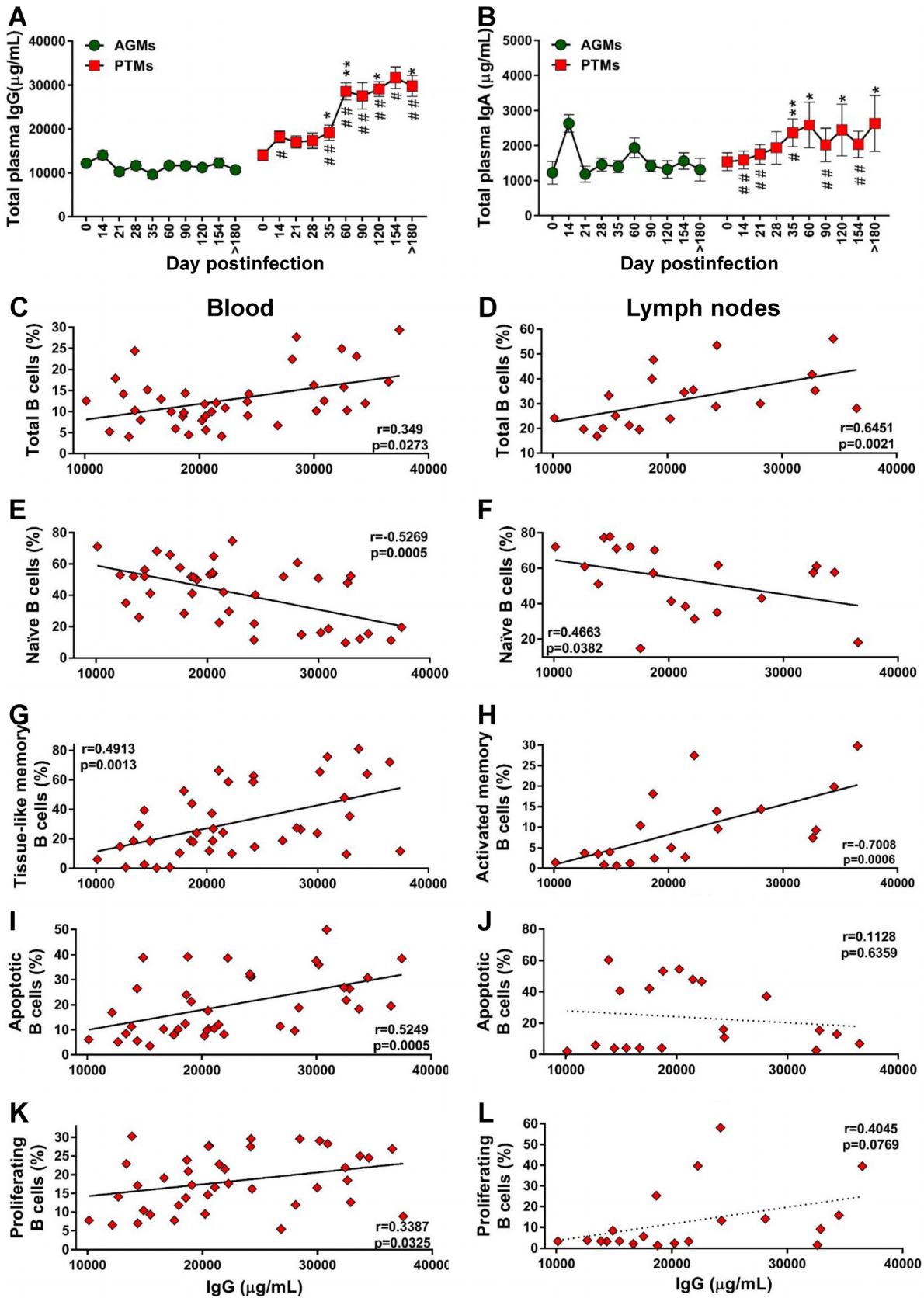
FIG 10 Assessment of the relationship between B cell dysfunction and overall humoral immune response over the course of progressive SIVsab infection of AGMs and nonprogressive SIVsab infection of PTMs. (A and B) Total levels of IgG (A) and total IgA (B) in AGMs and PTMs. Dotted lines mark the baseline levels of the different cell subsets. The Mann-Whitney U test was used to assess significance. Error bars

antibody avidity and conformation ratio—in both SIVsab-infected AGMs and PTMs (Fig. 11E and F). Similar profiles of maturation were observed in PTMs and AGMs, although antibody avidity was lower in AGMs than in PTMs at individual time points midmaturation (35 to 180 dpi) (Fig. 11E). The overall kinetics of avidity development were similar in AGMs and PTMs, but the PTMs showed a more rapid antibody maturation than AGMs. On the other hand, the conformational epitope recognition by Env-specific antibodies was very different between progressive and nonprogressive hosts ($P =$ 0.009) (Fig. 11F), with AGMs evolving from low to high conformation ratios and PTMs evolving from high to low conformation ratios, showing a pattern typically expected of SIV-infected animals. Multiple-comparison analysis indicated that the conformation ratio curve of the PTMs was significantly different from that of the AGMs (Fig. 11F).

DISCUSSION

There is a renewed interest in the role of B cells in the pathogenesis of HIV infection, fueled by studies showing that humoral immune responses may be central to an effective preventive and therapeutic HIV vaccine and for cure research (66–71). HIV type 1 (HIV-1) infection is associated with profound alterations of the B cell compartment (72) which may play a pivotal role in rapid disease progression (41, 44), as depletion of circulating B cells and low Ab responses are associated with progression to AIDS (73, 74).

To assess the contribution of B cell dysfunction to HIV/SIV disease progression, we compared and contrasted pathogenic and nonpathogenic models with regard to the dynamics of B cells and memory subsets, i.e., their levels of immune activation, apoptosis, exhaustion, and homing to the intestine. This allowed us to define specific B cell-related changes which might impact disease progression in the pathogenic SIV infection.

While the baseline levels of total B cells were similar in the two species, species-specific differences could be identified with regard to the memory B cell subsets: higher levels of tissue-like memory B cells and activated memory B cells in PTMs, lower levels of mucosal naive B cells in AGMs, and lower levels of mucosal resting and tissue-like memory B cells in PTMs. Thus, the frequencies of B cell subsets are significantly different between the pathogenic and the nonpathogenic models in the tissue compartments critical for virus replication, CD4$^+$ T cell depletion, and persistent immune activation and inflammation. However, the cross-sectional analysis did not permit any conclusion on whether such differences are critical for SIV pathogenesis or whether they just represent innate differences between the two species. Therefore, we next compared the dynamics of the B cells and subsets during the course of SIV infection in the two species and report that B cell loss is specifically associated with the pathogenic SIV infection. Conversely, in the nonpathogenic SIV infection, B cells are maintained at virtually the baseline levels in circulation while rapidly increasing in both the LNs and intestine. Our data thus suggest that early B cell loss during pathogenic infection may contribute to disease progression, while their involvement at tissue sites may be beneficial in the nonpathogenic SIV infection.

Loss of total memory B cells (2–4), imbalances in B cell subsets (42, 45, 75–77), and tissue-specific impairment of total B cell trafficking and functions, together with a

FIG 10 Legend (Continued)

correspond to standard errors of the means. Significant changes from the preinfection baseline levels are indicated as follows: *, $P < 0.05$; **, $P < 0.01$; and ***, $P < 0.001$. Significant differences between pathogenic and nonpathogenic species at same time point are indicated as follows: #, $P < 0.05$; ##, $P < 0.01$; and ###, $P < 0.001$. Significant positive correlations were established during the pathogenic SIV infection of PTMs between the levels of total IgG and total (C) and tissue-like memory (G) B cells from circulation (C) and total (D) and activated (H) B cells from the lymph nodes (D). Negative correlations between were established during the pathogenic SIV infection of PTMs between the levels of total IgG and the naive B cells from the peripheral blood (E) and lymph nodes (F). Significant positive correlation between the levels of total IgG and the levels of apoptotic B cells (I) and proliferating B cells (K) from peripheral blood and only trends for a negative correlation with the levels of apoptotic B cells (J) and for a positive correlation with the levels of proliferating B cells (L) from the lymph nodes were established. Relationships between the levels of total B cells and subsets, apoptotic and proliferating B cells from blood and lymph nodes, and total IgG were assessed using the Spearman rank correlation test. Significant correlations and positive or negative trends are illustrated by solid and dotted lines, respectively; P and Spearman rank correlation (r) value are shown.
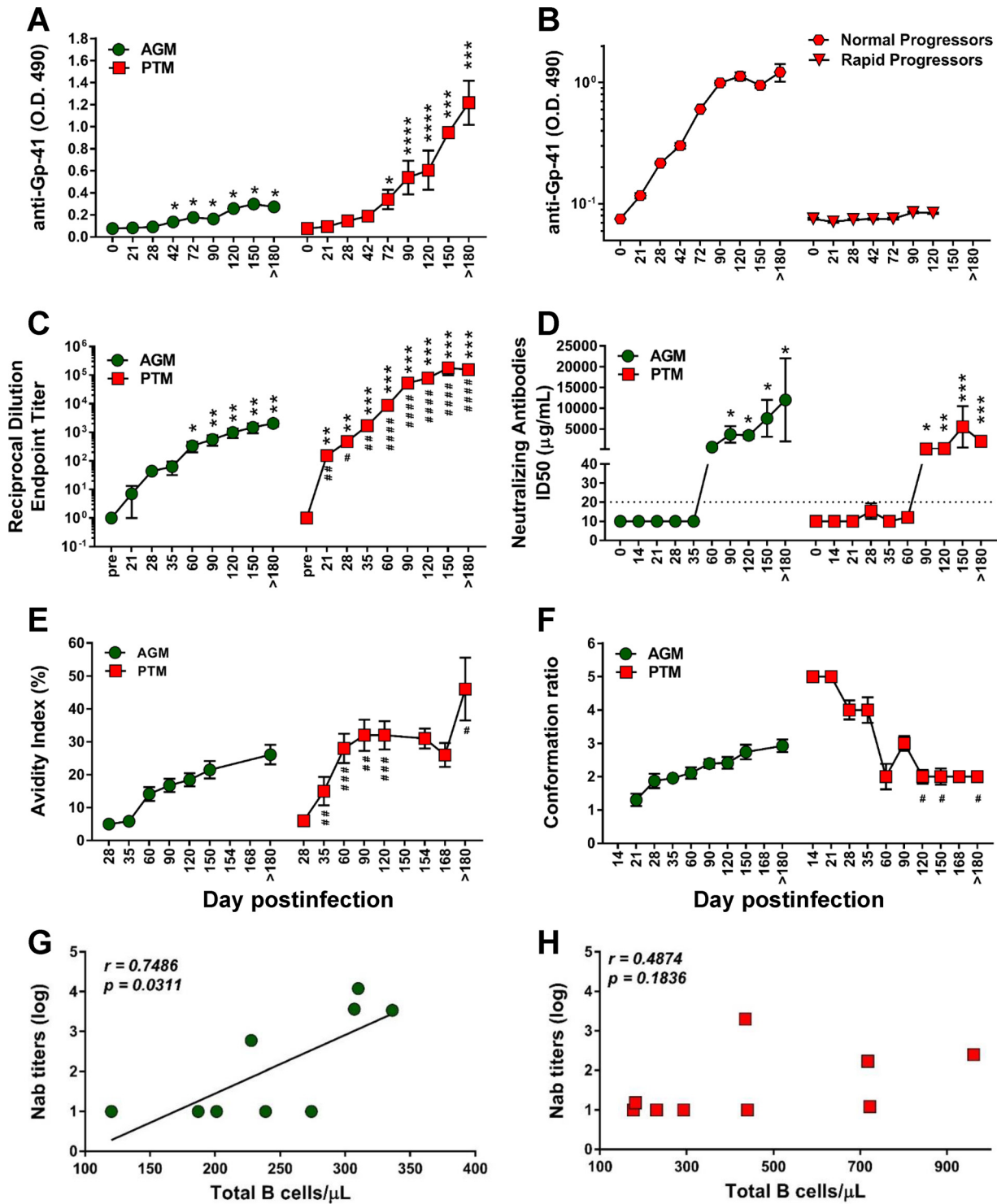
FIG 11 Antibody responses and antibody maturation profiles over the course of progressive SIVsab infection of AGMs and nonprogressive SIVsab infection of PTMs. (A) Anti-gp41 titers in AGMs and PTMs; (B) anti-gp41 antibody titers in normal progressor versus rapid progressor PTMs; (C) mean of endpoint titers of the highest reciprocal dilution; (D) neutralization antibodies titers; (E) mean avidity index; (F) mean conformation ratio. The Mann-Whitney U test was used to determine significance. Error bars correspond to standard errors of means. Significant differences compared to baseline values before infection are indicated as follows: *, $P < 0.05$; **, $P < 0.01$; ***, $P < 0.001$; and ****, $P < 0.0001$. Significant differences between AGMs and PTMs for the same time point are indicated as follows: #, $P < 0.05$; ##, $P < 0.01$; ###, $P < 0.001$; and ####, $P < 0.0001$. (G) Significant positive correlation between total peripheral B cells and production of neutralizing antibodies in AGMs (green circles). (H) Lack of correlation between the levels of total B cells and production of neutralizing antibodies in PTMs (red squares). Relationships between the levels of neutralizing antibodies and absolute counts of the total B cells were assessed using the Spearman rank correlation test. Significant correlations are represented by solid line; P and Spearman rank correlation (r) values are shown.

generalized and steady memory B cell loss in secondary lymphoid organs (45), occur in progressive HIV/SIV infections. We therefore compared the dynamics of naive, resting, activated, and tissue-like memory B cells from blood, LNs, and gut from SIV-infected PTMs and AGMs and established that the SIV-associated B cell dysfunction is characterized by loss of naive B cells, loss of resting memory B cells, increases of the activated B cells, and increases of the tissue-like memory B cells in circulation.

While the loss of circulating naive B cells was previously reported to occur in HIV/SIV infection (78), we show here that it is specifically associated with pathogenic SIV infection, as it does not occur in the nonpathogenic AGM model. Similarly, while previous studies reported the loss of memory B cells in chronically progressive HIV and SIV infections (42, 51, 52, 75, 79, 80), we report that resting memory B cells are massively redistributed to the gut during the pathogenic SIV infection of PTMs, which may explain their depletion from circulation. The different dynamics of resting memory B cells and their different trafficking patterns between pathogenic and nonpathogenic infections are other key findings of our study. The increase of the activated B cells in PTMs and in all studied compartments may contribute to chronic immune activation, the main driver of progression to AIDS (42, 51, 52, 81, 82). In contrast to previous studies with SIVmac-infected RMs that failed to identify any significant change of the tissue-like memory B cells associated with SIV infection (42, 51, 52), but in agreement with studies showing that they accumulate in circulation in HIV-infected patients (83), we found that this B cell subset is increased in circulation in SIVsab-infected PTMs. The difference with previous macaque studies may rely on the use in this study of the highly susceptible PTMs and a tier 2 virus, while studies with RMs employed the highly neutralization-resistant SIVmac.

Finally, we report that while circulating B cells are virtually restored to preinfection levels during chronic pathogenic SIV infection, restoration is mainly due to an expansion of the exhausted, virus-specific B cells, i.e., activated memory cells and tissue-like memory B cells (83). Their dominance during chronic HIV/SIV infection may contribute to the inefficiency of the antibody responses (72, 81).

These numerous differences between the pathogenic and nonpathogenic infections with regard to dynamics of the memory B cell subsets point to their role in the pathogenesis of HIV/SIV infections, suggesting that monitoring B cells may be a reliable approach for assessing disease progression.

We also report that changes in Breg frequency, which positively correlate with markers of HIV disease progression, such as the viral loads (VLs) and chronic immune activation, are specifically associated with the pathogenic SIV infection. Breg expansion might contribute to suppression of T cell effector functions either via the IL-10 and PD-L1 pathway or by attenuated proliferation of anti-HIV CD8$^+$ T cell effector subsets (53). Breg secretion of IL-10 (56–60) may also contribute to viral persistence (84) through suppression of T cell effector function (56, 57), and in our study, increased frequency of circulating B cells expressing IL-10 occurred only in the pathogenic infection. Therefore, our results are in agreement with previous studies (54, 55) reporting Breg involvement in disease progression. The precise mechanism through which Bregs impact SIV pathogenesis remains, however, unclear, as the immune responses are of similar magnitudes in the pathogenic and nonpathogenic SIV infections (8).

The mechanisms of B cell depletion during HIV/SIV infection are not completely understood; their reduction in circulation and increase in tissues of the PTMs suggest B cell mobilization to lymphoid sites during the pathogenic infection. We compared the changes in homing markers on the B cell subsets between pathogenic and nonpathogenic SIV infections, particularly the expression of the gut-homing marker $\alpha4\beta7$ integrin (85, 86), and we confirm that B cell loss from circulation may be due to their redistribution to the gut.

Circulating B cells may be also lost during SIV infection through cell death. As they cannot be infected by HIV/SIV and depleted through HIV/SIV killing, B cell reduced survival during infection likely occurs through apoptosis (45, 87). In our study, increased levels of apoptotic B cells in circulation and LNs and at the mucosal sites were specifically

associated with the pathogenic SIV infection and correlated with B cell activation, suggesting that apoptosis is likely involved in B cell loss.

Chronic immune activation is the main factor driving the progression of HIV infection to AIDS (1, 88). The ability of natural hosts to maintain low levels of T cell and myeloid dendritic cell (mDC) immune activation contributes to their resistance to SIV disease progression (2, 18, 89). Therefore, we investigated whether the natural hosts of SIV are also able to control B cell activation. We report that B cell activation occurred only at the transition from acute to chronic stage of infection (likely when the AGMs mounted the humoral immune responses), in stark contrast to the very early T cell activation observed in the PTMs (23). During the chronic SIV infection, the patterns of B cell activation were similar to those of the T cells, being resolved in the natural host while remaining increased throughout the follow-up in all the tissue compartments without a positive impact on the clinical course of SIV infection in the pathogenic model. Therefore, our results suggest that B cell activation contributes to the persistent inflammation that drives progression to AIDS (90).

To understand the mechanism of SIV-associated B cell activation, we assessed TLR-2 expression on B cells. TLR signaling plays an important role in microbial translocation (MT) (30, 91). Upon TLR-2, TLR-7, and TLR-9 activation, proliferative B cell responses can be detected in the follicular and marginal zone in the LNs (14, 92). B cell ligation of TLRs downregulates integrin receptor expression, leading to their redistribution from the marginal zone of spleen to circulation, LNs, and spleen follicles (93) and potent priming for Ig secretion (14, 36, 92, 94). We report that upon SIV infection, the levels of TLR-2 significantly increased only in the pathogenic model. This is not surprising, as TLR-2 binding to a wide range of microbial products translocated from the gut (91) may contribute to B cell activation (30, 95). Conversely, in chronically infected AGMs, the absence of microbial translocation may be the reason for the lack of TLR-2 overexpression. We therefore concluded that the mucosal damage specific to SIV/HIV infection contributes to B cell activation in a similar manner to that by which it drives T cell activation.

The generation and maintenance of memory of B cell responses in the LN microenvironment are governed by the Tfh cells (64, 96): Tfh cell accumulation is accompanied by B cell expansion and hypergammaglobulinemia in both HIV (97) and SIV (51, 98) infections. Tfh cells significantly expanded in the LNs in response to SIV infection in both progressive and nonprogressive hosts. The higher Tfh cell increase observed in PTMs during the chronic SIV infection may be a cause of abnormal Ab production in SIV infection, in agreement with recent studies with both NHPs (51, 98) and HIV-infected subjects (96, 97).

Finally, to establish whether B cell dysfunction impacts humoral immunity, we performed a thorough characterization of the humoral immune responses and their maturation. We first interrogated whether the loss of total B cells in progressive species impacts the overall humoral immunity. Surprisingly, we found that in spite of the observed B cell dysfunction, PTMs secrete significantly larger amounts of total IgG and IgA than AGMs. The study of relationships between total antibodies and the frequencies of total, apoptotic, and proliferating total B cells identified correlations only in PTMs. Furthermore, naive B cells were negatively correlated with the total IgG, probably due to the increased apoptosis and differentiation in specific anti-SIV memory B cell subsets. The total IgG levels were also negatively correlated with activated circulating memory B cells and positively correlated with the exhausted tissue-like memory B cells. Therefore, our results suggest that the majority of circulating antibodies produced during SIV infection in PTMs are secreted by activated, apoptotic, and exhausted B cells.

The anti-SIVsab antibody titers were higher in PTMs than in AGMs, probably as a result of the higher antigenic stimulation. Surprisingly, more than half of the rapid progressor PTMs did not have detectable anti-gp41 antibodies, as a result of a defective humoral immune response which could contribute either to the rapid progression or to the higher antigenic burden and antibody complexation masking the humoral immune responses (99).

We did not find any significant difference in the NAb profiles between pathogenic and nonpathogenic models, which led us to conclude that the levels of neutralizing antibodies do not significantly impact SIV disease outcome.

We next assessed the maturation of humoral immune responses in the two models by measuring antibody avidity and conformation ratio. Low antibody avidity of non-neutralizing antibodies is associated with poor protective efficacy (100, 101), while high avidity correlates with reduced better control of viremia (102). Protective efficacy of the humoral immune responses requires antibody maturation, i.e., high avidity and preferential recognition of conformational epitopes (103, 104). Comparison of the conformation ratio identified similar profiles of maturation between the pathogenic and the nonpathogenic SIV infections. The overall kinetics of avidity development were similar between AGMs and PTMs, yet the AGMs showed a delayed maturation compared to that in PTMs, suggesting that an earlier antibody maturation is not sufficient to improve clinical outcome. On the other hand, the conformational epitope recognition evolved from low to high conformation ratios in AGMs, similar to the pattern observed in HIV-infected patients, and from high to low conformation ratios in PTMs, following a pattern typically expected of SIV-infected NHPs (105). Taken together, our results show that in AGMs, unlike the pathogenic SIV infections, epitope recognition starts out at a higher level of linear epitopes, with increasing recognition of conformational epitopes over time. The patterns of early antibody recognition of more conformational epitopes and increasing recognition of linear epitopes over time characteristic to pathogenic SIV infection may thus be one of the factors behind the high susceptibility to disease progression.

In conclusion, by comparing and contrasting the B cell dynamics in blood and tissues in NHP models of progressive and nonprogressive SIV infections, we showed that B cell dysfunction defined by loss of total and memory B cells, increases in the circulating levels of tissue-like B cells and Bregs as well as increases of the B cell recruitment to the gut, B cell activation, and apoptosis is specifically associated with the pathogenic SIV infection, being absent during the nonpathogenic SIV infection. The observed changes in the B cell population were not correlated with production of neutralizing antibodies, the levels of which were similar in the two models. Yet rapid progressive infection is associated with a severe impairment in SIV-specific antibody production. While our study did not identify major differences in avidity and maturation between the pathogenic and nonpathogenic SIV infection, we found a major difference in conformational epitope recognition, with the nonpathogenic infection being characterized by an evolution from low to high conformations. These differences should be considered in designing immunization strategies aimed at preventing HIV disease progression.

MATERIALS AND METHODS

Ethics statement. All the NHPs included in this study were housed and maintained at the RIDC Park animal facility of the University of Pittsburgh according to the standards of the Association for Assessment and Accreditation of Laboratory Animal Care (AAALAC) International. Experiments presented here were approved by the University of Pittsburgh Institutional Animal Care and Use Committee (IACUC), the studies being covered by the IACUC protocols 0907039/12080831 (Animal Model for SIV Infection Control, approved in 2009 and renewed in 2012) and 0911844/12121250 (Pathogenesis of SIV in African Green Monkeys, approved in 2009 and renewed in 2012).

The animals were fed and housed according to regulations set forth by the Animal Welfare Act and the *Guide for the Care and Use of Laboratory Animals* (106, 107). All the animals included in this study were socially housed (paired) indoor in stainless steel cages, had a 12-h/12-h light/dark cycle, and were fed twice daily; water was provided *ad libitum*. The animals were given various toys and feeding enrichment. In addition, the animals were observed twice daily and any signs of disease or discomfort were reported to the veterinary staff for evaluation. For sample collection, animals were anesthetized with 10 mg/kg (of body weight) of ketamine hydrochloride (Park-Davis, Morris Plains, NJ) or 0.7 mg/kg of tiletamine hydrochloride and zolazepan (Telazol; Fort Dodge Animal Health, Fort Dodge, IA) injected intramuscularly. At the completion of the study or when they reached the AIDS-defining clinical endpoints, the animals were sacrificed by intravenous administration of barbiturates prior to the onset of any clinical signs of disease.

Animals and infections. Our study included a total of 40 AGMs and 29 PTMs. Different animals were used for different experiments carried out in this study. The AGMs were intravenously infected with

TABLE 1 Antibodies used for flow cytometry assay[a]

Marker	Clone	Fluorochrome	Company
CD3	SP34-2	Pacific Blue	BD Pharmingen
CD4	L200	APC	BD Pharmingen
CD8	3B5	PE-Texas Red	Invitrogen
CD20	2H7	APC-H7	BD Pharmingen
CD21	B-ly4	PE-Cy5	BD Pharmingen
CD24	ML5	PerCP-Cy5.5	BD Bioscience
CD27	M-T271	APC	BD Pharmingen
CXCR5 (CD185)	MU5UBEE	PE-Cy7	eBioscience
ICOS (CD278)	C398.4A	PerCP5.5	BioLegend
PD-1 (CD279)	eBioJ (J105)	PE	eBioscience
Annexin V	NA	FITC	BD Pharmingen
Bcl-6	K112-91	Alexa Fluor 488	BD Pharmingen
IL-10	JES3-9D7	Alexa Fluor 647	eBioscience
Ki-67	B56	FITC	BD Pharmingen
PD-L1	M1H1	PE-Cy7	eBioscience
TLR-2	T2.5	FITC	eBioscience
Viability dye	NA	Blue fluorescent reactive dye	Life Technologies

[a]APC, allophycocyanin; PE, phycoerythrin; PerCP, peridinin-chlorophyll protein; FITC, fluorescein
isothiocyanate; NA, not applicable.

plasma equivalent to 300 50% tissue culture infectious doses ($TCID_{50}$) of SIVsab92018 (108). The PTMs received intravenously plasma equivalent to 300 $TCID_{50}$ of SIVsabBH66 (109).

Four AGMs and 13 PTMs were used in a prospective study to assess (i) the dynamics of total and memory B cell subsets, B cell apoptosis, and immune activation status in blood, lymph nodes (LNs), and intestine; (ii) the dynamics of CD4$^+$ Tfh cells; and (iii) the dynamics of binding anti-gp41 and neutralizing antibodies (NAbs). The follow-up of NHPs in this group ranged between 1 week preinfection and up to 300 days postinfection (dpi) or until progression to AIDS. Animals were closely clinically monitored throughout the follow-up. Plasma VLs were quantified by real time-PCR as previously described (25, 108).

Additionally, to better support the findings of the prospective study, we have included samples collected at key time points of SIVsab infection from historical studies. Thus, 14 AGMs and 20 PTMs were used to monitor B regulatory cells (Bregs), B cell expression of IL-10, and TLR-2, and homing to the intestine.

Sampling. For the prospective study, blood, axillary/mesenteric LNs and intestinal biopsy specimens were collected as described previously (18, 110), prior to and after infection. The sampling schedule was as follows: whole blood was collected prior to infection (preinfection), twice per week during the first 2 weeks after SIVsab infection (at 4, 8, 10, and 14 dpi), weekly for the next 2 weeks (21 and 28 dpi), bimonthly for the next 2 months (42, 72, and 90 dpi), and either at the completion of the follow-up (300 dpi) or at the AIDS stage. Axillary LNs were collected prior to infection and at 4, 8, 14, 42, and 180 dpi. Additional mesenteric LNs were collected prior to infection and at 8 and 180 dpi. Intestinal biopsy specimens were collected prior to infection and at 8, 42, and 72 dpi. Intestinal resections (5 to 10 cm) were surgically performed prior to infection, during acute infection (8 dpi), and during chronic infection (180 dpi), as previously described (18, 25, 110). Additional intestinal samples were collected at the necropsy. Peripheral blood mononuclear cells (PBMCs) and mononuclear cells from the LNs and intestine were isolated as described previously (18, 36).

Antibodies and flow cytometry. Cells isolated from blood, axillary LNs, and intestine were immunophenotyped by flow cytometry. Briefly, 1×10^6 to 2×10^6 cells were stained with viability dye (blue dye; Life Technologies) and incubated for 15 min in the dark at room temperature. The cells were then washed with phosphate-buffered saline (PBS) and stained for 30 min in the dark at room temperature using a combination of antibodies (Table 1) appropriate for the identification of different B cell subsets and a combination of isotype and fluorescence-minus-one controls. Stained cells were washed in 1$\times$ PBS, fixed with 2% paraformaldehyde solution (PFA), and stored at 4°C prior to acquisition. A minimum of 100,000 CD20 or 250,000 live CD3 cells were acquired with FACSDiva software v.8.0. Acquired cells were analyzed using FlowJo 7.6.5 software.

Assessment of apoptosis and proliferation status of the B cells and subsets. Viable cells stained as described above were washed with 1$\times$ PBS and incubated with 1$\times$ annexin V buffer binding for 20 min or fixed with 2% PFA. Cells were then washed once with PBS and stained with anti-annexin V-fluorescein isothiocyanate (FITC) monoclonal antibody (MAb) or permeabilized with a solution containing 0.1% saponin and incubated for 30 min at room temperature in the dark. Permeabilized cells were then stained with an anti-Ki-67-FITC MAb (clone B56) (BD Pharmingen) for intracellular detection of Ki-67. Cells were then washed with 1$\times$ PBS, fixed with 2% PFA, and stored at 4°C prior to the acquisition. B cells (CD20^{pos}) expressing annexin V or Ki-67 were defined as apoptotic and proliferating B cells, respectively.

Tfh CD4$^+$ T cell staining. To assess the frequency of Tfh CD4$^+$ T cells, 2×10^6 cells from axillary and mesenteric LNs were stained with an amine-reactive fixable dead-cell dye (Invitrogen, Grand Island, NY), as described above, washed once with PBS plus 2% newborn calf serum (NCS; Atlanta Biological Inc.,

Flowery Branch, GA), and stained with appropriate antibodies (Table 1) to select the Tfh $CD4^+$ cell population. Cells were then washed with PBS plus 2% NCS, fixed with 2% PFA, and stored at 4°C. All samples were analyzed in a four-laser BD LSRII (BD Bioscience, San Jose, CA) flow cytometer. A minimum of 250,000 live CD3 cells were acquired with FACSDiva software, and FlowJo 7.6.5 software was used to analyze the populations.

Breg staining. To assess the frequency of Bregs, 2×10^6 PBMCs were stained with an amine-reactive fixable dead-cell dye (Invitrogen, Grand Island, NY), as described above, washed once with PBS plus 2% NCS (Atlanta Biological Inc., Flowery Branch, GA), and stained with appropriate antibodies (Table 1) to select Bregs. Cells were then washed with PBS plus 2% NCS, fixed with 2% PFA, and stored at 4°C. All samples were analyzed in a four-laser BD LSRII (BD Bioscience, San Jose, CA) flow cytometer. A minimum of 100,000 live CD20 cells were acquired with FACSDiva software and FlowJo 7.6.5 software for Breg analyses.

Monitoring of the anti-gp41 binding Ab. Enzyme-linked immunosorbent assay (ELISA) was performed to measure serum binding Abs to a peptide mapping the immunodominant region gp41, as previously described (65). Absorbance values (optical density [OD]) were read at 492 nm, and the cutoff to discriminate negative values was arbitrarily established at an OD of 0.2.

Serum NAb. SIVsab neutralizing Abs (NAbs) were measured using a SIVsab92018-specific neutralization assay, as previously described (5). Briefly, an SIVsab-specific molecularly cloned Env-pseudotyped virus containing full-length gp160 of SIVsab92018 (clone 28) was prepared as described previously (111). Neutralization titers were then measured as 50% reductions in luciferase reporter gene expression in TZM-bl cells, as reported previously (5).

Total IgG and IgA in plasma. Plasma samples were tested for total IgG and total IgA by ELISA using commercial kits for IgG and IgA (Life Diagnostic, Inc., PA), per the manufacturer's instructions. The results, expressed as micrograms per milliliter of immunoglobulin, were extrapolated from a standard curve.

Characterization of SIV envelope glycoprotein-specific antibodies by ConA ELISA. The reactivity of serum samples to SIVsab native envelope proteins was determined in a series of quantitative and qualitative concanavalin A (ConA) ELISAs, as described previously (112). Briefly, SIVsab92018 virions which had been Triton disrupted as described previously (113) were captured for 1 h at room temperature onto Immulon 2HB microtiter plates (Fisher Scientific, Pittsburgh, PA) coated with ConA (Sigma, St. Louis, MO). Following ConA capture, plates were washed with PBS and blocked by the addition of 5% dried milk in PBS (Blotto) for 1 h at room temperature. Serum samples were serially diluted 2× in Blotto and incubated for 1 h at room temperature. Following extensive washing, peroxidase-conjugated anti-monkey IgG, whole molecule (Sigma), was diluted in Blotto, added to each well, and incubated for 1 h at room temperature. After a final washing, plates were incubated with TM Blue substrate (Sigma) for 20 min at room temperature, color was developed by the addition of 1 N sulfuric acid, and plates were read at 450 nm using an automated plate reader. Endpoint titers were determined as the last 2× dilution that yielded an OD twice that of normal monkey serum at the lowest dilution (1:50) or an OD of 0.100, whichever was greater. Serum dilutions were selected in the linear range of the endpoint titer curve for qualitative assays of Ab avidity index and conformation ratio. Ab avidity was determined by measuring the stability of the Ag-Ab complexes to 8 M urea and is expressed as follows: percent Ab avidity index = (OD of wells washed with 8 M urea/OD of wells washed with PBS) × 100. Serum Abs with avidity index values of <30% are designated low-avidity Abs, those with values between 30 and 50% are designated moderate-avidity Abs, and those with values of >50% are considered high-avidity Abs. Conformational dependence, or the specificity for conformational viral envelope glycoprotein determinants compared to that of linear envelope determinants, was determined by measuring the reactivity to native versus denatured envelope proteins, where a ratio of >1 reflects predominant reactivity with native envelope proteins and a ratio of <1 reflects predominant reactivity with denatured envelope proteins. The results represent the averages from at least three independent experiments.

Statistical analyses. Data were expressed as averages ± standard errors of the means (SEM). We used the Mann-Whitney U test to assess significant changes during the follow-up. Results of statistical analyses were interpreted as significant if the P value was ≤0.05. Linear-relationship analyses between Breg-producing IL-10 versus percentage of Breg, between log NAb titers versus absolute counts of total B cells, and fold increase of total B cell proliferation versus fold increase of total B cell apoptosis were assessed by the Spearman rank correlation coefficient. All statistical analyses and graphs were prepared with GraphPad Prism software v.6.02 (GraphPad Software Inc., San Diego, CA).

REFERENCES

1. Pandrei I, Apetrei C. 2010. Where the wild things are: pathogenesis of SIV infection in African nonhuman primate hosts. Curr HIV/AIDS Rep 7:28–36. https://doi.org/10.1007/s11904-009-0034-8.

2. Pandrea I, Sodora DL, Silvestri G, Apetrei C. 2008. Into the wild: simian immunodeficiency virus (SIV) infection in natural hosts. Trends Immunol 29:419–428. https://doi.org/10.1016/j.it.2008.05.004.

3. VandeWoude S, Apetrei C. 2006. Going wild: lessons from naturally occurring T-lymphotropic lentiviruses. Clin Microbiol Rev 19:728–762. https://doi.org/10.1128/CMR.00009-06.

4. Silvestri G, Paiardini M, Pandrea I, Lederman MM, Sodora DL. 2007. Understanding the benign nature of SIV infection in natural hosts. J Clin Invest 117:3148–3154. https://doi.org/10.1172/JCI33034.

5. Gaufin T, Pattison M, Gautam R, Stoulig C, Dufour J, MacFarland J, Mandell D, Tatum C, Marx MH, Ribeiro RM, Montefiori D, Apetrei C, Pandrea I. 2009. Effect of B-cell depletion on viral replication and clinical outcome of simian immunodeficiency virus infection in a natural host. J Virol 83:10347–10357. https://doi.org/10.1128/JVI.00880-09.

6. Gaufin T, Ribeiro RM, Gautam R, Dufour J, Mandell D, Apetrei C, Pandrea I. 2010. Experimental depletion of CD8+ cells in acutely SIVagm-infected African green monkeys results in increased viral replication. Retrovirology 7:42. https://doi.org/10.1186/1742-4690-7-42.

7. Schmitz JE, Johnson RP, McClure HM, Manson KH, Wyand MS, Kuroda MJ, Lifton MA, Khunkhun RS, McEvers KJ, Gillis J, Piatak M, Lifson JD, Grosschupff G, Racz P, Tenner-Racz K, Rieber EP, Kuus-Reichel K, Gelman RS, Letvin NL, Montefiori DC, Ruprecht RM, Desrosiers RC, Reimann KA. 2005. Effect of CD8+ lymphocyte depletion on virus containment after simian immunodeficiency virus SIVmac251 challenge of live attenuated SIVmac239delta3-vaccinated rhesus macaques. J Virol 79:8131–8141. https://doi.org/10.1128/JVI.79.13.8131-8141.2005.

8. Dunham R, Pagliardini P, Gordon S, Sumpter B, Engram J, Moanna A, Paiardini M, Mandl JN, Lawson B, Garg S, McClure HM, Xu YX, Ibegbu C, Easley K, Katz N, Pandrea I, Apetrei C, Sodora DL, Staprans SI, Feinberg MB, Silvestri G. 2006. The AIDS resistance of naturally SIV-infected sooty mangabeys is independent of cellular immunity to the virus. Blood 108:209–217. https://doi.org/10.1182/blood-2005-12-4897.

9. Wang Z, Metcalf B, Ribeiro RM, McClure H, Kaur A. 2006. Th-1-type cytotoxic CD8+ T-lymphocyte responses to simian immunodeficiency virus (SIV) are a consistent feature of natural SIV infection in sooty mangabeys. J Virol 80:2771–2783. https://doi.org/10.1128/JVI.80.6.2771-2783.2006.

10. Bosinger SE, Li Q, Gordon SN, Klatt NR, Duan L, Xu L, Francella N, Sidahmed A, Smith AJ, Cramer EM, Zeng M, Masopust D, Carlis JV, Ran L, Vanderford TH, Paiardini M, Isett RB, Baldwin DA, Else JG, Staprans SI, Silvestri G, Haase AT, Kelvin DJ. 2009. Global genomic analysis reveals rapid control of a robust innate response in SIV-infected sooty mangabeys. J Clin Invest 119:3556–3572.

11. Chakrabarti LA, Lewin SR, Zhang L, Gettie A, Luckay A, Martin LN, Skulsky E, Ho DD, Cheng-Mayer C, Marx PA. 2000. Normal T-cell turnover in sooty mangabeys harboring active simian immunodeficiency virus infection. J Virol 74:1209–1223. https://doi.org/10.1128/JVI.74.3.1209-1223.2000.

12. Douek DC. 2003. Disrupting T-cell homeostasis: how HIV-1 infection causes disease. AIDS Rev 5:172–177.

13. Estes JD, Gordon SN, Zeng M, Chahroudi AM, Dunham RM, Staprans SI, Reilly CS, Silvestri G, Haase AT. 2008. Early resolution of acute immune activation and induction of PD-1 in SIV-infected sooty mangabeys distinguishes nonpathogenic from pathogenic infection in rhesus macaques. J Immunol 180:6798–6807. https://doi.org/10.4049/jimmunol.180.10.6798.

14. Giorgi JV, Hultin LE, McKeating JA, Johnson TD, Owens B, Jacobson LP, Shih R, Lewis J, Wiley DJ, Phair JP, Wolinsky SM, Detels R. 1999. Shorter survival in advanced human immunodeficiency virus type 1 infection is more closely associated with T lymphocyte activation than with plasma virus burden or virus chemokine coreceptor usage. J Infect Dis 179:859–870. https://doi.org/10.1086/314660.

15. Jacquelin B, Mayau V, Targat B, Liovat AS, Kunkel D, Petitjean G, Dillies MA, Roques P, Butor C, Silvestri G, Giavedoni LD, Lebon P, Barre-Sinoussi F, Benecke A, Muller-Trutwin MC. 2009. Nonpathogenic SIV infection of African green monkeys induces a strong but rapidly controlled type I IFN response. J Clin Invest 119:3544–3555.

16. Ma D, Jasinska AJ, Feyertag F, Wijewardana V, Kristoff J, He T, Raehtz K, Schmitt CA, Jung Y, Cramer JD, Dione M, Antonio M, Tracy R, Turner T, Robertson DL, Pandrea I, Freimer N, Apetrei C, International Vervet Research Consortium. 2014. Factors associated with siman immunodeficiency virus transmission in a natural African nonhuman primate host in the wild. J Virol 88:5687–5705. https://doi.org/10.1128/JVI.03606-13.

17. Pandrea I, Onanga R, Kornfeld C, Rouquet P, Bourry O, Clifford S, Telfer PT, Abernethy K, White LT, Ngari P, Muller-Trutwin M, Roques P, Marx PA, Simon F, Apetrei C. 2003. High levels of SIVmnd-1 replication in chronically infected Mandrillus sphinx. Virology 317:119–127. https://doi.org/10.1016/j.virol.2003.08.015.

18. Pandrea IV, Gautam R, Ribeiro RM, Brenchley JM, Butler IF, Pattison M, Rasmussen T, Marx PA, Silvestri G, Lackner AA, Perelson AS, Douek DC, Veazey RS, Apetrei C. 2007. Acute loss of intestinal CD4+ T cells is not predictive of simian immunodeficiency virus virulence. J Immunol 179:3035–3046. https://doi.org/10.4049/jimmunol.179.5.3035.

19. Beaumier CM, Harris LD, Goldstein S, Klatt NR, Whitted S, McGinty J, Apetrei C, Pandrea I, Hirsch VM, Brenchley JM. 2009. CD4 downregulation by memory CD4+ T cells in vivo renders African green monkeys resistant to progressive SIVagm infection. Nat Med 15:879–885. https://doi.org/10.1038/nm.1970.

20. Apetrei C, Gaufin T, Gautam R, Vinton C, Hirsch V, Lewis M, Brenchley J, Pandrea I. 2010. Pattern of SIVagm infection in patas monkeys suggests that host adaptation to simian immunodeficiency virus infection may result in resistance to infection and virus extinction. J Infect Dis 202(Suppl 3):S371–S376. https://doi.org/10.1086/655970.

21. Vinton C, Klatt NR, Harris LD, Briant JA, Sanders-Beer BE, Herbert R, Woodward R, Silvestri G, Pandrea I, Apetrei C, Hirsch VM, Brenchley JM. 2011. CD4-like immunological function by CD4- T cells in multiple natural hosts of simian immunodeficiency virus. J Virol 85:8702–8708. https://doi.org/10.1128/JVI.00332-11.

22. Milush JM, Mir KD, Sundaravaradan V, Gordon SN, Engram J, Cano CA, Reeves JD, Anton E, O'Neill E, Butler E, Hancock K, Cole KS, Brenchley JM, Else JG, Silvestri G, Sodora DL. 2011. Lack of clinical AIDS in SIV-infected sooty mangabeys with significant CD4+ T cell loss is associated with double-negative T cells. J Clin Invest 121:1102–1110. https://doi.org/10.1172/JCI44876.

23. Paiardini M, Muller-Trutwin M. 2013. HIV-associated chronic immune activation. Immunol Rev 254:78–101. https://doi.org/10.1111/imr.12079.

24. Pandrea I, Parrish NF, Raehtz K, Gaufin T, Barbian HJ, Ma D, Kristoff J, Gautam R, Zhong F, Haret-Richter GS, Trichel A, Shaw GM, Hahn BH, Apetrei C. 2012. Mucosal simian immunodeficiency virus transmission in African green monkeys: susceptibility to infection is proportional to target cell availability at mucosal sites. J Virol 86:4158–4168. https://doi.org/10.1128/JVI.07141-11.

25. Pandrea I, Ribeiro RM, Gautam R, Gaufin T, Pattison M, Barnes M, Monjure C, Stoulig C, Dufour J, Cyprian W, Silvestri G, Miller MD, Perelson AS, Apetrei C. 2008. Simian immunodeficiency virus SIVagm dynamics in African green monkeys. J Virol 82:3713–3724. https://doi.org/10.1128/JVI.02402-07.

26. Compton AA, Malik HS, Emerman M. 2013. Host gene evolution traces the evolutionary history of ancient primate lentiviruses. Philos Trans R Soc Lond B Biol Sci 368:20120496. https://doi.org/10.1098/rstb.2012.0496.

27. Ma D, Jasinska A, Kristoff J, Grobler JP, Turner T, Jung Y, Schmitt C, Raehtz K, Feyertag F, Martinez Sosa N, Wijewardana V, Burke DS, Robertson DL, Tracy R, Pandrea I, Freimer N, Apetrei C, International Vervet Research Consortium. 2013. SIVagm infection in wild African green monkeys from South Africa: epidemiology, natural history, and evolutionary considerations. PLoS Pathog 9:e1003011. https://doi.org/10.1371/journal.ppat.1003011.

28. Worobey M, Telfer P, Souquiere S, Hunter M, Coleman CA, Metzger MJ, Reed P, Makuwa M, Hearn G, Honarvar S, Roques P, Apetrei C, Kazanji M, Marx PA. 2010. Island biogeography reveals the deep history of SIV. Science 329:1487. https://doi.org/10.1126/science.1193550.

29. Brenchley JM, Paiardini M, Knox KS, Asher AI, Cervasi B, Asher TE, Scheinberg P, Price DA, Hage CA, Kholi LM, Khoruts A, Frank I, Else J, Schacker T, Silvestri G, Douek DC. 2008. Differential Th17 CD4 T-cell depletion in pathogenic and nonpathogenic lentiviral infections. Blood 112:2826–2835. https://doi.org/10.1182/blood-2008-05-159301.

30. Brenchley JM, Price DA, Schacker TW, Asher TE, Silvestri G, Rao S, Kazzaz Z, Bornstein E, Lambotte O, Altmann D, Blazar BR, Rodriguez B, Teixeira-Johnson L, Landay A, Martin JN, Hecht FM, Picker LJ, Lederman MM, Deeks SG, Douek DC. 2006. Microbial translocation is a cause of systemic immune activation in chronic HIV infection. Nat Med 12:1365–1371. https://doi.org/10.1038/nm1511.

31. Sandler NG, Wand H, Roque A, Law M, Nason MC, Nixon DE, Pedersen C, Ruxrungtham K, Lewin SR, Emery S, Neaton JD, Brenchley JM, Deeks SG, Sereti I, Douek DC, INSIGHT SMART Study Group. 2011. Plasma levels of soluble CD14 independently predict mortality in HIV infection. J Infect Dis 203:780–790. https://doi.org/10.1093/infdis/jiq118.

32. Brenchley JM, Silvestri G, Douek DC. 2010. Nonprogressive and progressive primate immunodeficiency lentivirus infections. Immunity 32:737–742. https://doi.org/10.1016/j.immuni.2010.06.004.

33. Brenchley JM, Paiardini M. 2011. Immunodeficiency lentiviral infections in natural and non-natural hosts. Blood 118:847–854. https://doi.org/10.1182/blood-2010-12-325936.

34. Paiardini M, Pandrea I, Apetrei C, Silvestri G. 2009. Lessons learned from the natural hosts of HIV-related viruses. Annu Rev Med 60:485–495. https://doi.org/10.1146/annurev.med.60.041807.123753.

35. Ansari AA, Mayne AE, Takahashi Y, Pattanapanyasat K. 2011. Incorporation of innate immune effector mechanisms in the formulation of a vaccine against HIV-1. Adv Exp Med Biol 780:143–159. https://doi.org/10.1007/978-1-4419-5632-3_12.

36. Wijewardana V, Kristoff J, Xu C, Ma D, Haret-Richter G, Stock JL, Policicchio BB, Mobley AD, Nusbaum R, Aamer H, Trichel A, Ribeiro RM, Apetrei C, Pandrea I. 2013. Kinetics of myeloid dendritic cell trafficking and activation: impact on progressive, nonprogressive and controlled SIV infections. PLoS Pathog 9:e1003600. https://doi.org/10.1371/journal.ppat.1003600.

37. Overbaugh J, Morris L. 2012. The antibody response against HIV-1. Cold Spring Harb Perspect Med 2:a007039. https://doi.org/10.1101/cshperspect.a007039.

38. Gautam R, Nishimura Y, Pegu A, Nason MC, Klein F, Gazumyan A, Golijanin J, Buckler-White A, Sadjadpour R, Wang K, Mankoff Z, Schmidt SD, Lifson JD, Mascola JR, Nussenzweig MC, Martin MA. 2016. A single injection of anti-HIV-1 antibodies protects against repeated SHIV challenges. Nature 533:105–109. https://doi.org/10.1038/nature17677.

39. Nishimura Y, Gautam R, Chun TW, Sadjadpour R, Foulds KE, Shingai M, Klein F, Gazumyan A, Golijanin J, Donaldson M, Donau OK, Plishka RJ, Buckler-White A, Seaman MS, Lifson JD, Koup RA, Fauci AS, Nussenzweig MC, Martin MA. 2017. Early antibody therapy can induce long-lasting immunity to SHIV. Nature 543:559–563. https://doi.org/10.1038/nature21435.

40. De Milito A. 2004. B lymphocyte dysfunctions in HIV infection. Curr HIV Res 2:11–21. https://doi.org/10.2174/1570162043485068.

41. Lane HC, Masur H, Edgar LC, Whalen G, Rook AH, Fauci AS. 1983. Abnormalities of B-cell activation and immunoregulation in patients with the acquired immunodeficiency syndrome. N Engl J Med 309:453–458. https://doi.org/10.1056/NEJM198308253090803.

42. Titanji K, Velu V, Chennareddi L, Vijay-Kumar M, Gewirtz AT, Freeman GJ, Amara RR. 2010. Acute depletion of activated memory B cells involves the PD-1 pathway in rapidly progressing SIV-infected macaques. J Clin Invest 120:3878–3890. https://doi.org/10.1172/JCI43271.

43. Chiodi F. 2010. New therapy to revert dysfunctional antibody responses during HIV-1 infection. J Clin Invest 120:3810–3813. https://doi.org/10.1172/JCI44872.

44. Buckner CM, Kardava L, Moir S. 2013. Evaluation of B cell function in patients with HIV. Curr Protoc Immunol Chapter 12:Unit 12.13.

45. Peruchon S, Chaoul N, Burelout C, Delache B, Brochard P, Laurent P, Cognasse F, Prevot S, Garraud O, Le Grand R, Richard Y. 2009. Tissue-specific B-cell dysfunction and generalized memory B-cell loss during acute SIV infection. PLoS One 4:e5966. https://doi.org/10.1371/journal.pone.0005966.

46. Poonia B, Pauza CD, Salvato MS. 2009. Role of the Fas/FasL pathway in HIV or SIV disease. Retrovirology 6:91. https://doi.org/10.1186/1742-4690-6-91.

47. Macatangay BJ, Rinaldo CR. 2009. PD-1 blockade: a promising immunotherapy for HIV? Cellscience 5:61–65.

48. Demberg T, Mohanram V, Venzon D, Robert-Guroff M. 2014. Phenotypes and distribution of mucosal memory B-cell populations in the SIV/SHIV rhesus macaque model. Clin Immunol 153:264–276. https://doi.org/10.1016/j.clim.2014.04.017.

49. Demberg T, Robert-Guroff M. 2015. B-cells and the use of non-human primates for evaluation of HIV vaccine candidates. Curr HIV Res 13:462–478. https://doi.org/10.2174/1570162X13666150724095339.

50. Thomas MA, Demberg T, Vargas-Inchaustegui DA, Xiao P, Tuero I, Venzon D, Weiss D, Treece J, Robert-Guroff M. 2014. Rhesus macaque rectal and duodenal tissues exhibit B-cell sub-populations distinct from peripheral blood that continuously secrete antigen-specific IgA in short-term explant cultures. Vaccine 32:872–880. https://doi.org/10.1016/j.vaccine.2013.12.014.

51. Hong JJ, Amancha PK, Rogers K, Ansari AA, Villinger F. 2012. Spatial alterations between CD4+ T follicular helper, B, and CD8+ T cells during simian immunodeficiency virus infection: T/B cell homeostasis, activation, and potential mechanism for viral escape. J Immunol 188:3247–3256. https://doi.org/10.4049/jimmunol.1103138.

52. Micci L, Ryan ES, Fromentin R, Bosinger SE, Harper JL, He T, Paganini S, Easley KA, Chahroudi A, Benne C, Gumber S, McGary CS, Rogers KA, Deleage C, Lucero C, Byrareddy SN, Apetrei C, Estes JD, Lifson JD, Piatak M, Jr, Chomont N, Villinger F, Silvestri G, Brenchley JM, Paiardini M. 2015. Interleukin-21 combined with ART reduces inflammation and viral reservoir in SIV-infected macaques. J Clin Invest https://doi.org/10.1172/JCI81400.

53. Siewe B, Stapleton JT, Martinson J, Keshavarzian A, Kazmi N, Demarais PM, French AL, Landay A. 2013. Regulatory B cell frequency correlates with markers of HIV disease progression and attenuates anti-HIV CD8+ T cell function in vitro. J Leukoc Biol 93:811–818. https://doi.org/10.1189/jlb.0912436.

54. Bouaziz JD, Calbo S, Maho-Vaillant M, Saussine A, Bagot M, Bensussan A, Musette P. 2010. IL-10 produced by activated human B cells regulates CD4+ T-cell activation in vitro. Eur J Immunol 40:2686–2691. https://doi.org/10.1002/eji.201040673.

55. Iwata Y, Matsushita T, Horikawa M, Dilillo DJ, Yanaba K, Venturi GM, Szabolcs PM, Bernstein SH, Magro CM, Williams AD, Hall RP, St Clair EW, Tedder TF. 2011. Characterization of a rare IL-10-competent B-cell subset in humans that parallels mouse regulatory B10 cells. Blood 117:530–541. https://doi.org/10.1182/blood-2010-07-294249.

56. Blair PA, Norena LY, Flores-Borja F, Rawlings DJ, Isenberg DA, Ehrenstein MR, Mauri C. 2010. CD19+ CD24hi CD38hi B cells exhibit regulatory capacity in healthy individuals but are functionally impaired in systemic lupus erythematosus patients. Immunity 32:129–140. https://doi.org/10.1016/j.immuni.2009.11.009.

57. Das A, Ellis G, Pallant C, Lopes AR, Khanna P, Peppa D, Chen A, Blair P, Dusheiko G, Gill U, Kennedy PT, Brunetto M, Lampertico P, Mauri C, Maini MK. 2012. IL-10-producing regulatory B cells in the pathogenesis of chronic hepatitis B virus infection. J Immunol 189:3925–3935. https://doi.org/10.4049/jimmunol.1103139.

58. DiLillo DJ, Weinberg JB, Yoshizaki A, Horikawa M, Bryant JM, Iwata Y, Matsushita T, Matta KM, Chen Y, Venturi GM, Russo G, Gockerman JP, Moore JO, Diehl LF, Volkheimer AD, Friedman DR, Lanasa MC, Hall RP, Tedder TF. 2013. Chronic lymphocytic leukemia and regulatory B cells share IL-10 competence and immunosuppressive function. Leukemia 27:170–182. https://doi.org/10.1038/leu.2012.165.

59. Horikawa M, Minard-Colin V, Matsushita T, Tedder TF. 2011. Regulatory B cell production of IL-10 inhibits lymphoma depletion during CD20 immunotherapy in mice. J Clin Invest 121:4268–4280. https://doi.org/10.1172/JCI59266.

60. Inoue S, Leitner WW, Golding B, Scott D. 2006. Inhibitory effects of B cells on antitumor immunity. Cancer Res 66:7741–7747. https://doi.org/10.1158/0008-5472.CAN-05-3766.

61. Chahroudi A, Bosinger SE, Vanderford TH, Paiardini M, Silvestri G. 2012. Natural SIV hosts: showing AIDS the door. Science 335:1188–1193. https://doi.org/10.1126/science.1217550.

62. Okoye AA, Picker LJ. 2013. CD4+ T-cell depletion in HIV infection: mechanisms of immunological failure. Immunol Rev 254:54–64. https://doi.org/10.1111/imr.12066.

63. Bekeredjian-Ding I, Jego G. 2009. Toll-like receptors—sentries in the B-cell response. Immunology 128:311–323. https://doi.org/10.1111/j.1365-2567.2009.03173.x.

64. Crotty S. 2011. Follicular helper CD4 T cells (TFH). Annu Rev Immunol 29:621–663. https://doi.org/10.1146/annurev-immunol-031210-101400.

65. Simon F, Souquiere S, Damond F, Kfutwah A, Makuwa M, Leroy E, Rouquet P, Berthier JL, Rigoulet J, Lecu A, Telfer PT, Pandrea I, Plantier JC, Barre-Sinoussi F, Roques P, Muller-Trutwin MC, Apetrei C. 2001. Synthetic peptide strategy for the detection of and discrimination

among highly divergent primate lentiviruses. AIDS Res Hum Retroviruses 17:937–952. https://doi.org/10.1089/088922201750290050.

66. Haynes BF, Montefiori DC. 2006. Aiming to induce broadly reactive neutralizing antibody responses with HIV-1 vaccine candidates. Expert Rev Vaccines 5:579–595. https://doi.org/10.1586/14760584.5.4.579.

67. Mascola JR. 2003. Defining the protective antibody response for HIV-1. Curr Mol Med 3:209–216. https://doi.org/10.2174/1566524033479799.

68. Montefiori DC, Morris L, Ferrari G, Mascola JR. 2007. Neutralizing and other antiviral antibodies in HIV-1 infection and vaccination. Curr Opin HIV AIDS 2:169–176. https://doi.org/10.1097/COH.0b013e3280ef691e.

69. Plotkin SA. 2008. Vaccines: correlates of vaccine-induced immunity. Clin Infect Dis 47:401–409. https://doi.org/10.1086/589862.

70. Lewis GK, Pazgier M, DeVico AL. 2017. Survivors remorse: antibody-mediated protection against HIV-1. Immunol Rev 275:271–284. https://doi.org/10.1111/imr.12510.

71. Rerks-Ngarm S, Pitisuttithum P, Nitayaphan S, Kaewkungwal J, Chiu J, Paris R, Premsri N, Namwat C, de Souza M, Adams E, Benenson M, Gurunathan S, Tartaglia J, McNeil JG, Francis DP, Stablein D, Birx DL, Chunsuttiwat S, Khamboonruang C, Thongcharoen P, Robb ML, Michael NL, Kunasol P, Kim JH, MOPH-TAVEG Investigators. 2009. Vaccination with ALVAC and AIDSVAX to prevent HIV-1 infection in Thailand. N Engl J Med 361:2209–2220. https://doi.org/10.1056/NEJMoa0908492.

72. Moir S, Fauci AS. 2009. B cells in HIV infection and disease. Nat Rev Immunol 9:235–245. https://doi.org/10.1038/nri2524.

73. Hart M, Steel A, Clark SA, Moyle G, Nelson M, Henderson DC, Wilson R, Gotch F, Gazzard B, Kelleher P. 2007. Loss of discrete memory B cell subsets is associated with impaired immunization responses in HIV-1 infection and may be a risk factor for invasive pneumococcal disease. J Immunol 178:8212–8220. https://doi.org/10.4049/jimmunol.178.12.8212.

74. Morris L, Binley JM, Clas BA, Bonhoeffer S, Astill TP, Kost R, Hurley A, Cao Y, Markowitz M, Ho DD, Moore JP. 1998. HIV-1 antigen-specific and -nonspecific B cell responses are sensitive to combination antiretroviral therapy. J Exp Med 188:233–245.

75. De Milito A, Morch C, Sonnerborg A, Chiodi F. 2001. Loss of memory (CD27) B lymphocytes in HIV-1 infection. AIDS 15:957–964. https://doi.org/10.1097/00002030-200105250-00003.

76. Titanji K, Chiodi F, Bellocco R, Schepis D, Osorio L, Tassandin C, Tambussi G, Grutzmeier S, Lopalco L, De Milito A. 2005. Primary HIV-1 infection sets the stage for important B lymphocyte dysfunctions. AIDS 19:1947–1955. https://doi.org/10.1097/01.aids.0000191231.54170.89.

77. Titanji K, De Milito A, Cagigi A, Thorstensson R, Grutzmeier S, Atlas A, Hejdeman B, Kroon FP, Lopalco L, Nilsson A, Chiodi F. 2006. Loss of memory B cells impairs maintenance of long-term serologic memory during HIV-1 infection. Blood 108:1580–1587. https://doi.org/10.1182/blood-2005-11-013383.

78. Kuhrt D, Faith SA, Leone A, Rohankedkar M, Sodora DL, Picker LJ, Cole KS. 2010. Evidence of early B-cell dysregulation in simian immunodeficiency virus infection: rapid depletion of naive and memory B-cell subsets with delayed reconstitution of the naive B-cell population. J Virol 84:2466–2476. https://doi.org/10.1128/JVI.01966-09.

79. Chong Y, Ikematsu H, Kikuchi K, Yamamoto M, Murata M, Nishimura M, Nabeshima S, Kashiwagi S, Hayashi J. 2004. Selective CD27+ (memory) B cell reduction and characteristic B cell alteration in drug-naive and HAART-treated HIV type 1-infected patients. AIDS Res Hum Retroviruses 20:219–226. https://doi.org/10.1089/088922204773004941.

80. Nagase H, Agematsu K, Kitano K, Takamoto M, Okubo Y, Komiyama A, Sugane K. 2001. Mechanism of hypergammaglobulinemia by HIV infection: circulating memory B-cell reduction with plasmacytosis. Clin Immunol 100:250–259. https://doi.org/10.1006/clim.2001.5054.

81. Moir S, Fauci AS. 2013. Insights into B cells and HIV-specific B-cell responses in HIV-infected individuals. Immunol Rev 254:207–224. https://doi.org/10.1111/imr.12067.

82. Pensieroso S, Galli L, Nozza S, Ruffin N, Castagna A, Tambussi G, Hejdeman B, Misciagna D, Riva A, Malnati M, Chiodi F, Scarlatti G. 2013. B-cell subset alterations and correlated factors in HIV-1 infection. AIDS 27:1209–1217. https://doi.org/10.1097/QAD.0b013e32835edc47.

83. Moir S, Ho J, Malaspina A, Wang W, DiPoto AC, O'Shea MA, Roby G, Kottilil S, Arthos J, Proschan MA, Chun TW, Fauci AS. 2008. Evidence for HIV-associated B cell exhaustion in a dysfunctional memory B cell compartment in HIV-infected viremic individuals. J Exp Med 205:1797–1805. https://doi.org/10.1084/jem.20072683.

84. Brooks DG, Trifilo MJ, Edelmann KH, Teyton L, McGavern DB, Oldstone MB. 2006. Interleukin-10 determines viral clearance or persistence in vivo. Nat Med 12:1301–1309. https://doi.org/10.1038/nm1492.

85. Arthos J, Cicala C, Martinelli E, Macleod K, Van Ryk D, Wei D, Xiao Z, Veenstra TD, Conrad TP, Lempicki RA, McLaughlin S, Pascuccio M, Gopaul R, McNally J, Cruz CC, Censoplano N, Chung E, Reitano KN, Kottilil S, Goode DJ, Fauci AS. 2008. HIV-1 envelope protein binds to and signals through integrin $\alpha 4\beta 7$, the gut mucosal homing receptor for peripheral T cells. Nat Immunol 9:301–309. https://doi.org/10.1038/ni1566.

86. Martinelli E, Veglia F, Goode D, Guerra-Perez N, Aravantinou M, Arthos J, Piatak M, Jr, Lifson JD, Blanchard J, Gettie A, Robbiani M. 2013. The frequency of $\alpha 4\beta 7^{high}$ memory CD4+ T cells correlates with susceptibility to rectal SIV infection. J Acquir Immune Defic Syndr 64:325–331. https://doi.org/10.1097/QAI.0b013e31829f6e1a.

87. van Grevenynghe J, Cubas RA, Noto A, DaFonseca S, He Z, Peretz Y, Filali-Mouhim A, Dupuy FP, Procopio FA, Chomont N, Balderas RS, Said EA, Boulassel MR, Tremblay CL, Routy JP, Sekaly RP, Haddad EK. 2011. Loss of memory B cells during chronic HIV infection is driven by Foxo3a- and TRAIL-mediated apoptosis. J Clin Invest 121:3877–3888. https://doi.org/10.1172/JCI59211.

88. Deeks SG, Tracy R, Douek DC. 2013. Systemic effects of inflammation on health during chronic HIV infection. Immunity 39:633–645. https://doi.org/10.1016/j.immuni.2013.10.001.

89. Pandrea I, Gaufin T, Brenchley JM, Gautam R, Monjure C, Gautam A, Coleman C, Lackner AA, Ribeiro RM, Douek DC, Apetrei C. 2008. Cutting edge: experimentally induced immune activation in natural hosts of simian immunodeficiency virus induces significant increases in viral replication and CD4+ T cell depletion. J Immunol 181:6687–6691. https://doi.org/10.4049/jimmunol.181.10.6687.

90. Agrawal S, Gupta S. 2011. TLR1/2, TLR7, and TLR9 signals directly activate human peripheral blood naive and memory B cell subsets to produce cytokines, chemokines, and hematopoietic growth factors. J Clin Immunol 31:89–98. https://doi.org/10.1007/s10875-010-9456-8.

91. Liu H, Komai-Koma M, Xu D, Liew FY. 2006. Toll-like receptor 2 signaling modulates the functions of CD4+ CD25+ regulatory T cells. Proc Natl Acad Sci U S A 103:7048–7053. https://doi.org/10.1073/pnas.0601554103.

92. Genestier L, Taillardet M, Mondiere P, Gheit H, Bella C, Defrance T. 2007. TLR agonists selectively promote terminal plasma cell differentiation of B cell subsets specialized in thymus-independent responses. J Immunol 178:7779–7786. https://doi.org/10.4049/jimmunol.178.12.7779.

93. Rawlings DJ, Schwartz MA, Jackson SW, Meyer-Bahlburg A. 2012. Integration of B cell responses through Toll-like receptors and antigen receptors. Nat Rev Immunol 12:282–294. https://doi.org/10.1038/nri3190.

94. Rubtsov AV, Swanson CL, Troy S, Strauch P, Pelanda R, Torres RM. 2008. TLR agonists promote marginal zone B cell activation and facilitate T-dependent IgM responses. J Immunol 180:3882–3888. https://doi.org/10.4049/jimmunol.180.6.3882.

95. Jiang W, Lederman MM, Hunt P, Sieg SF, Haley K, Rodriguez B, Landay A, Martin J, Sinclair E, Asher AI, Deeks SG, Douek DC, Brenchley JM. 2009. Plasma levels of bacterial DNA correlate with immune activation and the magnitude of immune restoration in persons with antiretroviral-treated HIV infection. J Infect Dis 199:1177–1185. https://doi.org/10.1086/597476.

96. Perreau M, Savoye AL, De Crignis E, Corpataux JM, Cubas R, Haddad EK, De Leval L, Graziosi C, Pantaleo G. 2013. Follicular helper T cells serve as the major CD4 T cell compartment for HIV-1 infection, replication, and production. J Exp Med 210:143–156. https://doi.org/10.1084/jem.20121932.

97. Lindqvist M, van Lunzen J, Soghoian DZ, Kuhl BD, Ranasinghe S, Kranias G, Flanders MD, Cutler S, Yudanin N, Muller MI, Davis I, Farber D, Hartjen P, Haag F, Alter G, Schulze zur Wiesch J, Streeck H. 2012. Expansion of HIV-specific T follicular helper cells in chronic HIV infection. J Clin Invest 122:3271–3280. https://doi.org/10.1172/JCI64314.

98. Petrovas C, Yamamoto T, Gerner MY, Boswell KL, Wloka K, Smith EC, Ambrozak DR, Sandler NG, Timmer KJ, Sun X, Pan L, Poholek A, Rao SS, Brenchley JM, Alam SM, Tomaras GD, Roederer M, Douek DC, Seder RA, Germain RN, Haddad EK, Koup RA. 2012. CD4 T follicular helper cell dynamics during SIV infection. J Clin Invest 122:3281–3294. https://doi.org/10.1172/JCI63039.

99. Schmitz JE, Kuroda MJ, Santra S, Simon MA, Lifton MA, Lin W, Khunkhun R, Piatak M, Lifson JD, Grosschupff G, Gelman RS, Racz P, Tenner-Racz K, Mansfield KA, Letvin NL, Montefiori DC, Reimann KA. 2003.

Effect of humoral immune responses on controlling viremia during primary infection of rhesus monkeys with simian immunodeficiency virus. J Virol 77:2165–2173. https://doi.org/10.1128/JVI.77.3.2165-2173.2003.

100. Usinger WR, Lucas AH. 1999. Avidity as a determinant of the protective efficacy of human antibodies to pneumococcal capsular polysaccharides. Infect Immun 67:2366–2370.

101. Delgado MF, Coviello S, Monsalvo AC, Melendi GA, Hernandez JZ, Batalle JP, Diaz L, Trento A, Chang HY, Mitzner W, Ravetch J, Melero JA, Irusta PM, Polack FP. 2009. Lack of antibody affinity maturation due to poor Toll-like receptor stimulation leads to enhanced respiratory syncytial virus disease. Nat Med 15:34–41. https://doi.org/10.1038/nm.1894.

102. Zhao J, Lai L, Amara RR, Montefiori DC, Villinger F, Chennareddi L, Wyatt LS, Moss B, Robinson HL. 2009. Preclinical studies of human immunodeficiency virus/AIDS vaccines: inverse correlation between avidity of anti-Env antibodies and peak postchallenge viremia. J Virol 83:4102–4111. https://doi.org/10.1128/JVI.02173-08.

103. Craigo JK, Li F, Steckbeck JD, Durkin S, Howe L, Cook SJ, Issel C, Montelaro RC. 2005. Discerning an effective balance between equine infectious anemia virus attenuation and vaccine efficacy. J Virol 79:2666–2677. https://doi.org/10.1128/JVI.79.5.2666-2677.2005.

104. Tagmyer TL, Craigo JK, Cook SJ, Even DL, Issel CJ, Montelaro RC. 2008. Envelope determinants of equine infectious anemia virus vaccine protection and the effects of sequence variation on immune recognition. J Virol 82:4052–4063. https://doi.org/10.1128/JVI.02028-07.

105. Craigo JK, Montelaro RC. 2013. Lessons in AIDS vaccine development learned from studies of equine infectious, anemia virus infection and immunity. Viruses 5:2963–2976. https://doi.org/10.3390/v5122963.

106. National Research Council. 2011. Guide for the care and use of laboratory animals, 8th ed. National Academies Press, Washington, DC.

107. US Animal and Plant Health Inspection Service. 2005. Animal Welfare Act and animal welfare regulations. US Department of Agriculture, Animal and Plant Health Inspection Service, Washington, DC.

108. Pandrea I, Apetrei C, Dufour J, Dillon N, Barbercheck J, Metzger M, Jacquelin B, Bohm R, Marx PA, Barre-Sinoussi F, Hirsch VM, Muller-Trutwin MC, Lackner AA, Veazey RS. 2006. Simian immunodeficiency virus SIVagm.sab infection of Caribbean African green monkeys: a new model for the study of SIV pathogenesis in natural hosts. J Virol 80:4858–4867. https://doi.org/10.1128/JVI.80.10.4858-4867.2006.

109. Mandell DT, Kristoff J, Gaufin T, Gautam R, Ma D, Sandler N, Haret-Richter G, Xu C, Aamer H, Dufour J, Trichel A, Douek DC, Keele BF, Apetrei C, Pandrea I. 2014. Pathogenic features associated with increased virulence upon simian immunodeficiency virus cross-species transmission from natural hosts. J Virol 88:6778–6792. https://doi.org/10.1128/JVI.03785-13.

110. Gautam R, Gaufin T, Butler I, Gautam A, Barnes M, Mandell D, Pattison M, Tatum C, Macfarland J, Monjure C, Marx PA, Pandrea I, Apetrei C. 2009. Simian immunodeficiency virus SIVrcm, a unique CCR2-tropic virus, selectively depletes memory CD4+ T cells in pigtailed macaques through expanded coreceptor usage in vivo. J Virol 83:7894–7908. https://doi.org/10.1128/JVI.00444-09.

111. Montefiori DC. 2005. Evaluating neutralizing antibodies against HIV, SIV, and SHIV in luciferase reporter gene assays. Curr Protoc Immunol Chapter 12:Unit 12.11.

112. Cole KS, Rowles JL, Jagerski BA, Murphey-Corb M, Unangst T, Clements JE, Robinson J, Wyand MS, Desrosiers RC, Montelaro RC. 1997. Evolution of envelope-specific antibody responses in monkeys experimentally infected or immunized with simian immunodeficiency virus and its association with the development of protective immunity. J Virol 71:5069–5079.

113. Clements JE, Montelaro RC, Zink MC, Amedee AM, Miller S, Trichel AM, Jagerski B, Hauer D, Martin LN, Bohm RP, Murphey-Corb M. 1995. Cross-protective immune responses induced in rhesus macaques by immunization with attenuated macrophage-tropic simian immunodeficiency virus. J Virol 69:2737–2744.